

Streamflow Predictions of Hunza and Gilgit River Basins and its Impact on Hydro-Power Generation



By

Rehan Ahmad Parvaiz

(2019-NUST-MS-GIS-00320228)


**A thesis submitted in partial fulfillment of the requirements for the degree
of Master of Science in Remote Sensing and GIS**

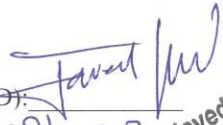
**Institute of Geographical Information Systems
School of Civil and Environmental Engineering
National University of Sciences & Technology
Islamabad, Pakistan**


August 2023


THESIS ACCEPTANCE CERTIFICATE

Certified that final copy of MS/MPhil thesis written by Rehan Ahmad Parvaiz (Registration No. MSRSGIS 0000320228), of Session 2019 (Institute of Geographical Information systems) has been vetted by undersigned, found complete in all respects as per NUST Statutes/Regulation, is free of plagiarism, errors, and mistakes and is accepted as partial fulfillment for award of MS/MPhil degree. It is further certified that necessary amendments as pointed out by GEC members of the scholar have also been incorporated in the said thesis.

Signature: 
Name of Supervisor: Dr Muhammad Azmat
Date: 29-08-2023

Signature (HOD): 
Date: 29/08/2023
Dr. Javed Iqbal
Professor & HOD IGIS, SCEE (NUST)
H-12, Islamabad

Signature (Associate Dean): 
Date: 29.8.2023
Dr. Ejaz Hussain
Associate Dean IGIS, SCEE (NUST)
H-12, ISLAMABAD

Signature (Principal & Dean SCEE): 
Date: 29 AUG 2023
PROF DR MUHAMMAD IRFAN
Principal & Dean
SCEE, NUST

ACADEMIC THESIS. DECLARATION OF AUTHORSHIP

I, **Rehan Ahmad Parvaiz**, declare that this thesis and the work presented in it are my own and have been generated by me as the result of my own original research.

“Streamflow Predictions of Hunza and Gilgit River Basins and its Impact on Hydro-Power Generation”

I confirm that.

1. This thesis is composed of my original work, and contains no material previously published or written by another person except where due reference has been made in the text.
2. Wherever any part of this thesis has previously been submitted for a degree or any other qualification at this or any other institution, it has been clearly stated.
3. I have acknowledged all main sources of help.
4. Where the thesis is based on work done by myself jointly with others, I have made clear exactly what was done by others and what I have contributed myself.
5. None of this work has been published before submission.
6. This work is not plagiarized under the HEC plagiarism policy.

Signed.



Date. : 29-08-2023

DEDICATION

“Dedicated to my Family who support me in all moments of life.”

Thanks for their love, care, and motivation since the start of my studies and all those who encouraged me and prayed for me for the completion of this thesis

ACKNOWLEDGEMENTS

All praises to almighty Allah who to whom everything belongs and to whom we all will return. First, I would like to give special thanks to my supervisor Dr. Muhammad Azmat for his devoted guidance throughout my research period and thankful to my examination committee members Dr. Ejaz Hussain, and Dr. Shakil Ahmad. Their support, guidance and suggestions helped me a lot. I am also thankful to the IGIS, NUST and all administration, which supported me to do research in this developing and growing field.

I am also grateful for the direct or indirect, considerate support and help of those whom I didn't mention here. I am thankful for their sincere efforts.

I am also thankful to the administration of Nusrat Jahan College, whose continuous support helped me a lot to complete this research. Without their support and help it could be difficult to reach completion.

Finally, my gratitude to my family for their trust in me and providing me with moral and financial support to acquire my ambition, I just can't thank them enough.

Rehan Ahmad Parvaiz

TABLE OF CONTENTS

ACCEPTANCE CERTIFICATE	i
ACADEMIC THESIS. DECLARATION OF AUTHORSHIP	ii
DEDICATION	iii
ACKNOWLEDGEMENTS	iv
LIST OF FIGURES	vii
LIST OF TABLES	viii
ABSTRACT	ix
Chapter 1: INTRODUCTION	1
1.1 Background	1
1.2 Rationale:	8
1.3 Objectives.....	9
Chapter 2: LITERATURE REVIEW	10
Chapter 3: MATERIALS and METHODS	18
3.1 Study area.....	18
3.1.1 Gilgit River Basin	18
3.1.2 Hunza River Basin:	20
3.2 Datasets	21
3.2.1 Daily streamflow data:	22
3.2.2 Weather Data:.....	22
3.2.3 Climate Projections:.....	22
3.2.4 Digital Elevation model (ASTER GDEM):.....	24
3.2.5 Snow cover data:.....	24
3.3 Methodology	26
3.3.1 Hydro Modelling:.....	26

3.3.2	Snowmelt Runoff Model (SRM)	27
3.3.3	Structure of Model:	28
Chapter 4: RESULTS and DISCUSSION		30
4.1	Analysis of snow cover area.....	30
4.1.1	Winter Months (December - March):	30
4.1.2	Transition Period (April - May):	30
4.1.3	Warmer Months (June - October):	30
4.1.4	Late Autumn (November):	32
4.1.5	Zonal Snow cover analysis.	32
4.2	Analysis of Runoff Simulations	34
4.3	Assessment of Model Efficiency Tests	38
4.3.1	Coefficient of determination R^2 :	38
4.3.2	Volume Difference in Percentage (Dv%).....	40
4.3.3	Nash-Sutcliffe efficiency Test (NSE).....	40
4.4	Comparison of Streamflow with Trends in SCA	41
4.5	Sensitivity analysis.....	41
4.6	Analysis of future projections:	43
4.7	Impact of Future Projections on Stream Flows.....	43
4.7.1	Contribution of Snow melt on Stream Flows:	47
4.8	Flow Duration Curves	50
4.9	Hydro-Power generation estimation:	53
Chapter 5: CONCLUSION and RECOMMENDATIONS		56
5.1	Conclusion.....	56
REFERENCES		58

LIST OF FIGURES

Figure 3.1. Study area map showing Hunza and Gilgit basin.....	19
Figure 3.2. DEM showing area elevation zones.	25
Figure 3.3. Showing methodology flowchart.	29
Figure 4.1. Change in Snow cover area over Gilgit and Hunza river basin during each month of a year.....	31
Figure 4.3. Zone wise trends SCA for years 2013-14.....	33
Figure 4.2. Zone wise trends SCA for years 2009-10.....	33
Figure 4.5. Measured vs Computed runoff for calibration period 2010.	35
Figure 4.4. Measured vs Computed runoff for calibration period 2009.	35
Figure 4.7. Measured vs Computed runoff for validation period 2014.	36
Figure 4.6. Measured vs Computed runoff for validation period 2013.	36
Figure 4.8. Comparison of streamflow with trends in SCA.	42
Figure 4.9. Future projections for change in minimum temperature under SSP2-45.....	44
Figure 4.10. Future projections for change in maximum temperature under SSP2-45.	44
Figure 4.11. Future projections for change in minimum temperature under SSP5-8.5.	45
Figure 4.12. Future projections for change in maximum temperature under SSP5-8.5.	45
Figure 4.13. Future projections for change in precipitation under SSP2-4.5.	46
Figure 4.14. Future projections for change in precipitation under SSP5-8.5.	46
Figure 4.15. Projected streamflow under SSP2-4.5.....	48
Figure 4.16. Projected streamflow under SSP5-8.5.....	48
Figure 4.17. Projected streamflow by contribution of snow and glacier melt under climate change scenario SSP2-4.5.....	51
Figure 4.18. Projected streamflow by contribution of snow and glacier melt under climate change scenario SSP5-8.5.....	51
Figure 4.19. Flow duration curve for future stream flows under climate change scenarios SSP2-4.5.....	54
Figure 4.20. Flow duration curve for future stream flows under climate change scenarios SSP5-8.5.....	54

LIST OF TABELS

Table 3.1. Showing the list of datasets used to conduct this study.	23
Table 4.1. Showing zone wise parameter values.	Error! Bookmark not defined.
Table 4.2. Model efficiency results	39
Table 4.3. Projected streamflow under current and future climate change scenarios.....	49
Table 4.4. The contribution of snowmelt on projected streamflow under current and future climate change scenarios.....	52
Table 4.5. Expected Hydropower generation under current and future climate change scenario SSP2-4.5.....	55
Table 4.6. Expected Hydropower generation under current and future climate change scenario SSP5-8.5.....	55

ABSTRACT

The alteration of regional water availability due to forthcoming climatic changes will stand as a critical societal impact. These hydrological shifts will exert comprehensive influences on various dimensions of human welfare, encompassing agricultural productivity, energy consumption, flood management, provisioning of municipal and industrial water, as well as the oversight of aquatic life and wildlife. The aim of this study was to assess the snow and glacier melt contribution in overall river flows of Hunza and Gilgit River Basins using hydrological Modeling technique under current and future climate change scenarios and analysis of the consequences of climate change impacts on hydropower generation using flow duration curves. The use of (SRM) snowmelt runoff model was satisfactory to compute the daily discharges of Hunza and Gilgit rivers. Modis Mod10a1 provides daily snow cover data with 500m spatial resolution used in this study to extract region's snow cover. Hydro-climatic data was another major input for model, for this purpose the ERA5 satellite data provided by ECMWF was used to extract temperature and precipitation values on daily basis. After calibration of model for years 2009 and 2010, it was successfully validated for years 2013-2014. The Nash-Sutcliffe model efficiency coefficient was ranging from 0.85 to 0.89 and difference in volume was ranging from 1.09% to 2.91%. The shared socioeconomic pathways SSP2-45 and SSP5-85 scenarios of the Coupled Model Intercomparison Project 6 (CMIP6) was used to analyze the impacts of climate change on overall stream flows of Gilgit and Hunza river catchments. The application of future climate change scenarios suggests that by increasing mean temperature values the streamflow will increase 44% under SSP2 and a huge increase of 105% as 21st century reaches to end. The flow duration curves show the 62% increase in power generation for 50% exceedance of time by using estimated stream flows. The findings presented here can be used with any type of stream and hydrological system at the power plant.

INTRODUCTION

1.1 Background

The alteration of regional water availability due to forthcoming climatic changes will stand as a critical societal impact. These hydrological shifts will exert comprehensive influences on various dimensions of human welfare, encompassing agricultural productivity, energy consumption, flood management, provisioning of municipal and industrial water, as well as the oversight of aquatic life and wildlife. To exemplify, regions anticipating elevated runoff will necessitate expanded reservoir spillways and drainage systems, while locales expecting diminished runoff must prioritize heightened water storage for supply purposes. The substantial significance of water within both societal and ecological contexts underscores the indispensable requirement for comprehending the potential ramifications of global climate fluctuations on local water provisions. In an era marked by mounting populations, the repercussions of global warming, and the detrimental impact of pollution on water quality, the significance of Earth's most precious resource, water, is consistently escalating. This intensifying importance stems from the expanding demands across residential, industrial, and agricultural sectors. (Yelesliere et al., 2018) acknowledge these trends. The principal origin of freshwater rests in precipitation, manifested through rainfall or snowfall. Notably, mountains experience substantial levels of both rain and snow, rendering them the primary wellspring of fresh water. The pivotal role of snow-covered regions lies in the phenomenon of snow-induced runoff, catalyzed by snowmelt, which predominantly initiates during the spring season coinciding with amplified requirements for water (Krishna et al., 2011) More than one-sixth of the global population relies on water sourced originating by snowmelt for their water supply. The prevailing and foremost challenge confronting the world today is the

phenomenon of climate change and its intertwined aspect of global warming. The repercussions of this environmental transformation on water supplies are notably diverse and often unpredictable. As we progress toward the conclusion of the current century, substantial alterations in climate patterns are anticipated due to the persistent escalation of greenhouse gas emissions. The trajectory of climate change is an unequivocal certainty, driven by the escalating global mean temperatures and the profound alterations inflicted upon the atmosphere's chemical composition by human activities. The elevated mountainous terrain has borne a substantial brunt of the repercussions of global climate change in the recent decades. Notably, snow, glaciers, and permafrost exhibit heightened vulnerability to shifts in climatic factors due to their closeness to melting thresholds. Indeed, one of the most conspicuous outcomes of rising temperatures is the transformation in the presence of ice and its cascading effects on the physical dynamics of elevated mountain systems (Haberli, 1990).

Snowmelt and glacier-melt derived water sources are indispensable for over one-sixth of the global populace's water provisioning. The prevailing paramount challenge confronting the world pertains to the events of global climate change. This environmental upheaval's repercussions on water supplies, specifically, exhibit a marked propensity for diversity and unpredictability. The trajectory towards the century's conclusion portends substantial climate alterations, attributed to the relentless surge in greenhouse gas emissions. The inevitable continuity of climate evolution is a foregone conclusion, substantiated by the ascending global mean temperatures, propelled by profound alterations in the atmospheric chemical composition induced by human activities. Over recent decades, the elevated mountainous milieu has borne a pronounced impact of global climate change. Notably, the transformative effects of shifts in air conditions hold resonance for snow, glaciers, and permafrost due to their proximity to critical melting thresholds. In essence, one of the

most perceptible outcomes of escalating temperatures could manifest as alterations in ice occurrences and their cascading ramifications for the physical dynamics of elevated mountain systems (Haberli, 1990). The upward trajectory of temperatures, coupled with shifts in precipitation patterns, amplifies the hydrological cycle, leading to increased stream flow volume and its temporal distribution across the year. This phenomenon, however, gives rise to notable water stress (Houghton et al., 2021). As indicated by (Kundzewicz et al., 2007) the discharge within glacier-fed rivers is anticipated to experience an initial upsurge, followed by a decline over the ensuing decades due to the gradual diminution of ice storage. This underscores the pivotal role of temperature fluctuations in governing the allocation of precipitation. Precipitation, whether in the form of snow, rain, glacier melting, or a combination thereof, significantly contributes to freshwater reserves. The reduction in glacier coverage across mountainous regions has become pronounced due to ongoing global warming trends. A recent investigation by the United States Geological Survey, utilizing historical glacier data and imagery from NASA's TERRA satellite's ASTER instrument, indicates noteworthy reduction in the size of mountain glaciers within areas such as the Andes, the Himalayas, the Alps, and the Pyrenees during the last ten years. (wessels et al., 2002) These findings align with the widespread conclusions drawn from various glacier studies conducted globally, all of which highlight the rapid pace of glacial retreat in recent times. (Meier, 1997) conducted a comprehensive study that encompassed more than 200 glaciers and found a global retreat in glaciated area ranging from 6,000 and 8,000 km² between 1960's and 1990's. (Hoelzle, 2001) from the organization which monitors the Glaciers of the World (WGMS) noted that observations spanning the past century unmistakably demonstrate a global-scale reduction in mountain glaciers. Their findings indicate that this trend reached its zenith in the early 20th century, followed by a resurgence in glacier growth around 1950. However, during the 1980s, the pace of

glacier retreat escalated once again, exceeding the scope of pre-industrial variability. The IPCC's Second Assessment Report in 1996, based on comprehensive scientific research, forecasted that approximately 25% of the total mass of mountain glaciers worldwide might vanish by 2050, and as much as 50% by the year 2100. (Rees and Collins, 2004). IPCC's 2007 report further highlighted that in certain moist tropical areas and high latitudes, annual average river discharge and water availability might witness a rise of 10–40% by the mid-century, while in select dry regions and mid-latitudes, they could decline by 10–30%. Presently, more than 16% of the global population lives in areas that depend on meltwater from major mountain ranges for sustenance; nevertheless, projections indicate a decline in water reservoirs stocked in glaciers and snow cover throughout the 21st century. Situated between 24° and 38° N and 61° and 78° E, Pakistan stands as one of the many developing nations in the region. The country heavily relies on snow and ice melt in its mountainous areas to fill a significant portion of its freshwater supply. However, the susceptibility of this water source to climate variations introduces various potential impacts. Pakistan's vulnerability is heightened due to its substantial reliance on uninterrupted river flow for sustained water access and power generation. The Indus River, originating in northern Pakistan and terminating at the Arabian Sea in the south, forms a pivotal component of this system (Hayat et al., 2019). Given Pakistan's diverse climatic conditions, the ramifications of climate change could be particularly pronounced. The complex interaction between melting snow and glacier runoff within the Indus Basin bears great significance for the agricultural-based economy of the country (Archer et al., 2010)

The Indus Basin, a significant river basin in Asia, supplies over 70% of water to the Pakistan's dry and low-lying areas. (Mukhopadhyay et al., 2015) Anchored in the Hindukush-Karakoram and Himalaya (HKH) mountain ranges, the Indus River's sustenance chiefly relies on snow and glacial

meltwater (Adnan et al., 2017). The Indus River's water supply holds multifaceted importance, serving as a critical resource for irrigation, electricity generation, and a significant source of clean water for downstream populations (Immerzeel et al., 2009). The designation of the Hindukush-Karakoram-Himalaya (HKH) region as the "water tower of Asia" underscores its pivotal role, as warming trends in this area raise serious environmental concerns and garner substantial scientific attention. The far-reaching impacts of global climate change have deleterious effects on snow and glaciers within Pakistan's HKH domain, which contributes more than half to the total runoff of the Indus River basin (Ashraf et al., 2012). The evolving flow patterns, influenced by climate change and other factors, have the potential to intensify tensions between provinces. Downstream areas, particularly the Sindh province, face the dual challenges of reduced water availability during dry seasons and heightened flood risks in wet seasons. Over the past three decades, the HKH region has experienced an increase in temp of 1.5°C, twice the (0.7 °C) observed in further areas of the country (Rasul, 2012). This escalating temperature trend is anticipated to exert a discernible impact on snow cover dynamics, subsequently altering the temporal patterns of seasonal flows (Akhtar et al., 2008; Immerzeel et al., 2009). Since 1950, the glaciers in the HKH region have exhibited mass loss and recession, although these variations lack regional uniformity in their measurements (Immerzeel et al., 2010; Hewitt, 2011; Immerzeel et al., 2013). Anticipated within the next twenty to thirty years, the unprecedented melting of Himalayan glaciers is poised to result in extensive flooding followed by subsequent declines in river water supply (Parry, 2007). Flash floods in the Hindukush and western Himalayas are predominantly triggered by the swift thawing of snow accumulated during winter months (Xu et al., 2007). Climatic transformations exert a disproportionately adverse impact on runoff, especially in rivers reliant on snowmelt (Adam et al., 2009; Panday and Brown, 2010). Consequently, the simulation and prediction of streamflow hold

paramount importance, providing a crucial foundation for the handling and designing water resources. (Abudu et al., 2010). This approach facilitates the anticipation of alterations in basin discharge, offering valuable insights for water resource management and effectively mitigating flood risks associated with swiftly melting of snow.

For effective handling of water resources in such areas, comprehending snow processes is imperative. The dynamics of snow accumulation and melting exert significant influence over the water cycle of a substantial portion of Earth's land surface, (Adam et al., 2009). Moreover, accurate calculation of areas covered by snow serves as a obligatory for the calibration and validation of hydrological models and plays a pivotal role in forecasting seasonal flow patterns (Hasson et al., 2014). The Himalayan-Karakoram-Hindukush (HKH) region is characterized by rugged terrain, inaccessibility, and challenges in data collection, leading to a dearth of essential data for comprehensive exploration of higher-altitude hydrological processes (Hewitt et al., 2011); Adnan et al., 2017). Consequently, remote sensing data has emerged as a valuable resource in numerous studies aimed at understanding hydrological dynamics (Immerzeel et al., 2013; Tahir et al., 2016; (Hayat et al., 2019). Research pertaining to snow cover and the process of snowmelt has confirmed the appropriateness of utilizing data from the Moderate Resolution Imaging Spectroradiometer (MODIS) to assess the extent of snow cover in mountainous regions. Tekeli et al. (2005) conducted an evaluation of MODIS snow coverage against ground-based surveillance and found that the derived snow cover accurately reflects conditions in a rugged river basin. Several snowmelt forecasting models, such as SSARR, HEC-1, NWSRFS, PRMS, SWAT, and GAWSER, as well as the Snow Melt Runoff model (SRM), have been developed to address diverse hydrological scenarios. However, a significant proportion of these models require extensive data input and exhibit complexity in application (Stigter et al., 2017). Employing an energy balance model offers

a comprehensive framework for comprehending the intricate processes of snow and glacier melting. However, the efficacy of this model hinges on the availability of extensive data, which is typically lacking in high-elevation mountainous regions (Agarwal et al., 2014; Bash, 2014). The pursuit of mass balance studies has revealed that these approaches can be intricate and time-consuming (Zemp et al., 2009; Nuimura et al., 2011).

The Snow Melt Runoff model (SRM) has garnered widespread utilization in simulating and predicting runoff across more than 100 river basins globally. The model relies on inputs such as basin characteristics, hydro-meteorological data, and the percentage of snow-covered area, rendering it applicable to basins spanning diverse extents and altitudinal ranges (Martinec et al., 2008). (Immerzeel et al., 2009) demonstrated the accuracy of the SRM in predicting streamflow by integrating MODIS snow product data, particularly in areas dominated by snowmelt.

Projections concerning climate alterations derived from both regional and global climate models can be seamlessly incorporated into the SRM. This facilitates the investigation of the impact of climate change on snowmelt runoff dynamics (Immerzeel et al., 2009)

Top of Form Examining the intricate snow cover and hydrology within the challenging and imprecisely measured Himalayan-Karakoram-Hindukush (HKH) region presents considerable difficulties. There is an urgent imperative to investigate the potential impacts of diverse future climate scenarios on the hydrological dynamics of the Hindukush region, particularly due to the recurrent flooding events in Pakistan. Moreover, limited research exists that estimates snowmelt within the Hindukush area across varying climate change scenarios. Thus, a comprehensive study on snowmelt runoff at the sub-catchment level of the Hindukush region is crucial to enhance flood prediction capabilities, facilitate optimal water resource management, and effectively address irrigation requirements downstream.

Efficiently orchestrating the thawing snow patterns holds the promise of meeting the escalating demands for agriculture, municipal water supply, energy generation, flood mitigation, navigation, and recreational amenities (Loucks et al., 2017). The snow cover extent in basins profoundly influences the hydrological and climatological behavior of these regions. Vigilant monitoring of snow-related dynamics bears immense relevance for a spectrum of hydrological analyses, water resource assessments, management of mountain reservoirs, flood control, and hydropower production. Precisely estimating the rate and volume of water discharge originating from snowmelt is indispensable for the adept management of downstream water resources (Arian et al., 2016).

The central aim of this study is to evaluate the contributions of snow and glacier melt to the overall river flows within the Hunza and Gilgit River Basins using hydrological modeling techniques under prevailing and future climate change scenarios. Additionally, the investigation encompasses an analysis of the ramifications of climate change impacts on hydropower generation by utilizing flow duration curves. The selection of the Snow Melt Runoff model (SRM) for this study is substantiated by two key factors: firstly, the model's primary reliance on snow cover area extent, which can be accurately determined through satellite, aerial, or ground measurements, thus minimizing data input requirements. Secondly, a comprehensive study evaluating multiple models conducted by the World Meteorological Organization (WMO, 1986) underscores the SRM's position as the most optimal choice available.

1.2 Rationale:

It is needed to understand the contribution of snow and glacier melt in river flows of Hunza and Gilgit River Basins. The Snow and glacier melt have a significant impact on the overall river flows in the study area. The contribution of snow and glacier melt to river flows has changed over time

due to changing climate conditions. Changes in snow and glacier melt contributions could have significant consequences on the hydropower potential of the study area.

1.3 Objectives

The main objectives of this research were:

1. To assess the snow melt contribution in overall river flows of Hunza and Gilgit River Basins using hydrological Modeling technique under current and future climate change scenarios.
2. Analyzing the consequences of climate change impacts on hydropower generation using flow duration curves.

LITERATURE REVIEW

Pokhrel et al., (2014) conducted a specific study in 2014 in which they used two models, namely the SRM (Snowmelt Runoff Model) and GR4J (model for the simulation of runoff from lumped precipitation). Snow and glacier melting had a significant impact on the overall discharge. The SRM model outperformed the GR4J model in terms of performance. While the GR4J model does not show a substantial rise with this assumption, a significant influence on runoff was detected when the air temperature values were changed from 2°C to 4°C to check the impact of the changing climate. (Pokhrel et al., 2014)

Snowmelt runoff is the primary source of water in arid alpine locations. The fundamental issue in modeling snowmelt runoff in high altitude places is a paucity of gauge stations, particularly in big basins. Methods of interpolation substantially help in refining the precision of simulations as well as the description of hydrological behaviors of catchments for overcoming ambiguities in data of snowmelt runoff modeling. The SRM model was applied in a research investigation spanning the Kaidu River watershed. SRM was used in a study across the Kaidu River watershed. The SRM simulation record with temperature estimates demonstrated that temperature plays an important role in determining runoff owing to snowmelt. It also showed that temperature changes have a substantial impact on snowfall and snowmelt regimes because rising temperatures increase the intensity and rate of snowmelt during warm seasons, which changes the peaks and timing of runoff throughout the year. (Dou, Chen, Bao, & Li, 2011).

Covering an approximate expanse of 16,933 km², the glaciers in Pakistan contribute significantly to its geographical diversity. Within Pakistan's landscape are 108 peaks soaring above 6000 meters,

alongside multiple summits surpassing altitudes of 5000 and 4000 meters, which includes a representation among the world's top 14 independently located summits (Jilani et al., 2007).

The hydrological framework of Pakistan is profoundly shaped by the Indus River and its primary tributaries, namely the Kabul, Jhelum, Chenab, Ravi, and Sutlej rivers. This riverine network is aptly likened to a funnel, as diverse water sources converge at its upper reaches to form the unified Indus River, eventually merging into the Arabian Sea (Ali et al., 2009).

Integral to the water supply of the Indus River is the substantial contribution from glacier melt. The freshwater sourced from the melting of snow and ice serves as a vital lifeline for both irrigation practices and the generation of hydropower (Khalid et al., 2015). However, the reserves of frozen water are undergoing unprecedented depletion due to the escalating impacts of global warming, thereby triggering a notable increase in both the quantity and expanse of glacial lakes (Chaudhry et al., 2011).

This dynamic state of frozen water resources is influenced by the intricate interplay of climatic variables, resulting in annual and seasonal fluctuations in the extent of snow cover. These variations, in turn, wield direct influence over the availability of water resources (Ahmad et al., 2018) Over the past four decades, a multitude of models have been developed worldwide to characterize the intricate processes of snowmelt runoff. Among these, the Snowmelt Runoff Model (SRM) has emerged as a standout performer, effectively employed in more than a hundred catchments dispersed across diverse global regions (Rango, 1986) This model, when coupled with remote sensing data, has demonstrated its prowess in replicating daily streamflow patterns within catchments characterized by a snow-dominated environment. The versatility of SRM extends to mountain basins of varying sizes and elevations, rendering it an adaptable tool for simulation. Significantly, even in basins devoid of historical discharge and meteorological data, the SRM can

accurately estimate daily snowmelt discharge, provided the requisite input variables are available. The model's capacity to execute an uninterrupted run for an indefinite number of days, predicated upon a known or forecasted discharge value, adds to its utility.

The pivotal determinants of the SRM's efficacy encompass three primary variables: Snow Cover Area (SCA), temperature, and precipitation. Of these, MODIS furnishes essential spatial-temporal data encapsulating shifts in snow cover, a factor profoundly influencing the performance of the SRM (Kult et al., 2014).

Within the extensive body of literature, a multitude of studies have undertaken an assessment of the efficacy of the Snowmelt Runoff Model (SRM) in gauging streamflow simulations across diverse basins worldwide. An exemplary instance involves the selection of SRM to model and predict daily discharge for multiple basins within the Spanish Pyrenees (Gómez-Landesa & Rango, 2002). In this endeavor, the snow cover image is derived through a linear combination of NOAA channels 1 and 2. Employing area snow cover as a key input, real-time forecasts are generated using SRM. The outcomes from these SRM-based analyses significantly contributed to enhancing water resource management practices for hydropower companies operating in the Spanish Pyrenees. Similarly, the applicability of SRM was extended to the mountainous river basins of Nepal, where it showcased its potential in the planning and management of water resources (Dhami et al., 2018). Additionally, the adaptability of SRM was assessed within the upper Indus River basin. In a study focused on simulating runoff during the snowmelt season of 2004 in the upper Heihe River basin, the WinSRM version 1.10 was utilized (Li & Wang, 2008). The computed volume difference (DV) amounted to 7.124%, while the coefficient of determination (R^2) stood at 0.020. In the context of this basin, wherein snowmelt constitutes the sole source of runoff, the results underscored SRM's appropriateness for effectively modeling the intricate runoff dynamics.

To comprehensively assess the adaptability of SRM within a continental climate context, a scrutiny of its performance was conducted in the Gongnaisi river basin located in the western Tianshan Mountains (Ma & Cheng, 2003). Notably, this investigation revealed a noteworthy advancement, as snow coverage and the timing of snowmelt seasons exhibited an inclination toward earlier dates.

A pivotal contribution to the validation of snowmelt runoff simulations was achieved through an examination of the Beas River basin, situated at the Pandoh Dam in India (Prasad & Roy, 2005). In this endeavor, the basin's topography was meticulously subdivided into 12 elevation zones, each with a maximum elevation of 500 meters. Utilizing input parameters extracted from diverse sources such as existing maps, satellite data, meteorological records, and hydrological data, the measured and estimated runoffs displayed compelling consistency, affirming the efficacy of the model. Additionally, the application of SRM extended to the Astore River, a component of northern Pakistan's Upper Indus Basin, as investigated by Butt & Bilal (2011). This study further exemplified SRM's versatility and viability in simulating snowmelt runoff dynamics within distinct geographical contexts. To validate the effectiveness of a synergistic application involving the Snowmelt Runoff Model (SRM) and remote sensing data for the simulation of daily streamflow dynamics within snow-dominated catchments, a comprehensive examination was undertaken in the north-East region of Iran (Firouzi et al., 2016).

Central to the model's framework were Snow Cover Area (SCA), precipitation, and temperature, while spatial and temporal insights were harnessed through the utilization of MODIS 8-day composite snow cover imagery. The model's proficiency was gauged via the assessment of the volume difference (4.6%) and coefficient of determination (0.85%), indicating that meticulous parameter evaluation yields effective simulation outcomes. In a parallel endeavor, the Shyok River basin, a sub-catchment within the Upper Indus Basin (UIB), was investigated through an integrated

approach involving SRM and remotely sensed snow cover data (MOD10A2) to model snowmelt runoff patterns under present and future climatic scenarios (Tahir et al., 2019). The obtained results underscored SRM's capacity in adeptly reproducing the flow dynamics within the Shyok River.

Similarly, the application of SRM extended to the Sutlej basin, where snow-covered area (SCA) data sourced from remote sensing platforms such as NOAA, AVHRR, and MODIS were employed to estimate streamflow within the basin (Jain et al., 2012). Model calibration using a three-year dataset was supplemented by employing seasonal temperature lapse rates derived from land surface temperature maps, yielding appreciable enhancements in the model's predictive performance. Subsequently, an exploration was conducted within the Tamor river basin situated in the eastern Nepalese Himalaya, where three distinct climate scenarios were introduced as variables within the Snowmelt Runoff Model (SRM), aiming to scrutinize the repercussions of evolving climate conditions on the basin's hydrology (Panday et al., 2014). Upon subjecting the model to a scenario encompassing a 4°C rise in temperature and a 20% increase in precipitation, a remarkable surge in runoff volume by approximately 23% was observed, with streamflow surpassing present levels across all months. Conversely, a second scenario involving a 4°C temperature elevation exhibited a shift in snowmelt runoff patterns without significantly impacting flow volume. Meanwhile, maintaining temperatures at their current levels while augmenting precipitation by 20% led to a 15% escalation in runoff volume, primarily concentrated during the summer months. These outcomes underscore the compelling necessity for enhanced monitoring and modeling initiatives within the region to gain deeper insights into the ramifications of climate change on hydrology.

Furthermore, within the Gilgit River basin, the integration of SRM and MODIS facilitated the simulation of daily discharges and the computation of the snowmelt's influence on discharge

dynamics (Latif et al., 2019). This endeavor yielded results showcasing an average volume difference (DV) of -0.51 and an impressive Nash-Sutcliffe efficiency (NSE) of 0.81 when comparing observed and simulated flow patterns. However, the study also illuminated the model's susceptibility during high flow months, such as June, July, and August. This uncertainty stems from glacier-melt runoff, predominantly manifesting in August due to the glacier melting process.

Recent investigations highlight the utilization of various data sources and inputs within the Snowmelt Runoff Model (SRM) to achieve robust streamflow predictions in diverse catchments globally. Notably, these encompass Moderate Resolution Imaging Spectro-diameter (MODIS) products, alongside NOAA and Landsat TM products, Digital Elevation Model (DEM), and Normalized Difference Snow Index (NDSI). In addition, the integration of SRM with MODIS remote sensing snow cover products has enabled the simulation of daily discharge patterns within the Hunza river basin, facilitating an examination of the influence of climate change on these hydrological dynamics.

The outcomes derived from these efforts underline the effectiveness of SRM, particularly within the context of snow- and glacier-fed sub-catchments residing within the Upper Indus River Basin (Tahir et al., 2011). These findings collectively suggest that SRM holds significant potential for efficient application in regions characterized by intricate snow and glacier interactions, offering valuable insights into hydrological responses amidst changing climatic conditions. Multiple research endeavors underscore the advantageous capabilities of the Snowmelt Runoff Model (SRM) in forecasting short-term runoff and floods. A promising avenue for leveraging remote sensing data in the prediction of river inflow to the Krasnodar reservoir was examined (Georgievsky, 2009). Employing MODIS MOD10A2 eight-day composite snow cover data, essential remote sensing insights were harnessed, enabling the creation of maps detailing the

maximum extent of snow coverage across key river basins feeding the Krasnodar reservoir. This investigation illuminated SRM's adeptness in successfully estimating short-term runoff and endorsed its applicability in flood forecasting and water resource management within the research area (Haq, 2008).

Similarly, the Kabul River catchments witnessed the integration of the SRM model, incorporating daily precipitation, air temperature, discharge, and snow cover data as input variables (Rasouli et al., 2015). Model outcomes exhibited commendable agreement with measured daily discharge, substantiating the viability of SRM in estimating discharge within the snow-fed sub-catchment of the upper Kabul River basin, along with other mountainous basins in Afghanistan. Moreover, the reliability of SRM for predicting snowmelt runoff in ungauged snow-covered mountainous catchments was substantiated, particularly in the eastern region of the country through the utilization of MODIS snow cover maps (Tekeli et al., 2005). These results collectively establish SRM as a dependable tool for forecasting snowmelt runoff and simulating hydrological dynamics in various settings, including Turkey's basins. While the Snowmelt Runoff Model (SRM) offers significant advantages, it is not without limitations. Several investigations underscore the challenge posed by the scarcity of climate stations, particularly in regions with low snow density, where monitoring snowfall and snowmelt processes solely through meteorological data becomes intricate (Khan et al., 2016). To bridge these gaps, the integration of remotely sensed data for deriving snow maps has been proposed. Notably, certain findings suggest that SRM's effectiveness might diminish in snow-deficient areas.

A pertinent example of this can be observed in the examination of SRM's feasibility in simulating daily snowmelt runoff within an arid mountain watershed characterized by limited hydro-meteorological measurements (Li and Williams, 2008). This study tested the applicability of SRM

in such challenging settings, highlighting the need for careful consideration and adaptation of the model in regions where snow resources are scarce.

MATERIALS AND METHODS

3.1 Study area

The study area comprises of two River basins i.e., Gilgit and Hunza River, which are part of the mighty Upper Indus Basin (UIB). A brief description of both river basins is as under.

3.1.1 Gilgit River Basin

The Gilgit River basin, which has a large drainage area Figure (3.1), is situated in Pakistan's Gilgit-Baltistan region, on the eastern side of the Hindukush Range. This valley extends southeast before draining into the enormous Indus River. At the Alam Bridge hydrometric station, the river's discharge is constantly observed. Geographically, the basin is located between 35.80°N and 36.91°N latitudes and between 72.53°E and 74.70°E longitudes. From towering peaks that soar as high as 7,730 meters to low-lying plateaus that are 1,250 meters above sea level, the elevation within the basin varies widely (Ali, 2017). The basin's topography comprises diverse features, with a substantial portion of about 982 km² located at elevations exceeding 5,000 meters. A significant proportion of the basin, approximately 8%, is covered by glaciers, making up approximately 4% of the entire Upper Indus Basin's cryosphere extent. This icy domain is characterized by approximately 944 km² of clean glacier area and an additional 146 km² covered by debris. These glaciers play a vital role in maintaining the region's water resources, acting as natural reservoirs that release water during the warmer months. Throughout the year, the extent of snow-covered area (SCA) in the basin experiences significant variations. During the winter season, the average SCA reaches approximately 85%, whereas in the summer, this coverage diminishes considerably,

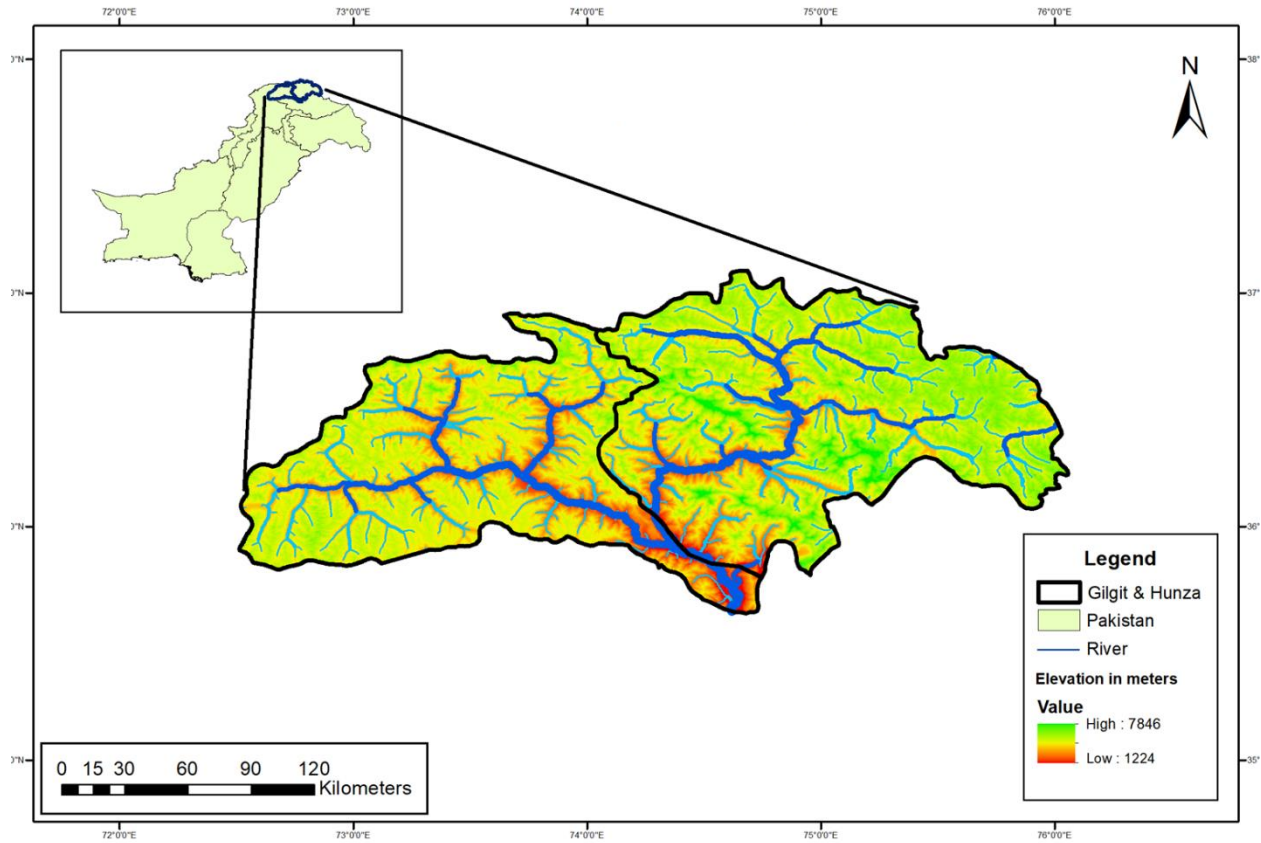


Figure 3.1. Study area map showing Hunza and Gilgit basin.

dropping to around 10% (Tahir, 2011). This seasonal fluctuation in SCA has significant implications for the timing and magnitude of snowmelt runoff, which, in turn, influences the river's flow and water availability downstream. Precipitation in the Gilgit River basin is contributed by two primary weather systems: westerly disturbances and the summer monsoon. The region receives rainfall and snowfall from westerly disturbances during the winter months. In contrast, the summer monsoon brings moisture-laden winds that lead to heavy rainfall in the basin, replenishing its water resources and supporting the ecological balance. The Gilgit River basin is home to an impressive number of glaciers and glacier lakes, adding to the basin's hydrological complexity. A total of 585 glaciers and 605 glacier lakes are scattered throughout the landscape. Among these glacier lakes, eight are identified as potentially dangerous due to the risk of glacial lake outburst floods (GLOFs), which can pose significant hazards to downstream communities and infrastructure (Amjad, 2023). Understanding the dynamics of glaciers, glacier lakes, and their interactions with the climate and hydrology is of paramount importance. As climate change continues to exert its influence on this sensitive region, accurate knowledge of the basin's cryosphere processes, and water resources is essential for sustainable water management, disaster risk reduction, and informed decision-making for the well-being of the communities that rely on the Gilgit River basin's resources.

3.1.2 Hunza River Basin:

The Hunza River catchment, covering a substantial drainage area Fig (2.1), is situated in the high-altitude central Karakoram region of Pakistan. Its geographical boundaries extend from 36.05°N latitude to 37.08°N latitude and 74.04°E longitude to 75.77°E longitude, encompassing a breathtaking landscape. The mean catchment elevation of the basin is approximately 4,631 meters, accentuating its high-altitude characteristics. The elevation within the basin exhibits a remarkable

range, spanning from 1,432 meters above sea level to towering peaks reaching as high as 7,849 meters. Within the basin, a vast portion of about 4,152 km² is covered by glaciers, signifying the significant cryosphere influence in the region. These glaciers serve as vital reservoirs of freshwater, supplying water to the river and contributing to the region's overall hydrology. The Hunza River basin has around 1,384 glaciers. It encompasses a clean glacier area of 3,673.04 km² and a debris-covered area of 479.56 km² (Ali, 2017). This delineation between clean ice and debris-covered ice helps to differentiate the glaciers' characteristics and their contributions to the basin's water resources. Throughout the year, the snow cover area (SCA) in the Hunza River basin experiences substantial fluctuations. In the winter season, the average SCA extends over approximately 80% of the basin's surface. However, as the warmer months arrive, this snow coverage recedes, leaving approximately 30% of the basin's area under snow. These seasonal variations in SCA play a pivotal role in the timing and magnitude of snowmelt runoff, ultimately influencing the river's discharge and water availability downstream. Given the significance of glaciers in the basin's hydrology, understanding their dynamics, characteristics, and responses to climate change is of paramount importance (Tahir, 2011). As climate variability continues to impact this ecologically sensitive region, studying the Hunza River basin's cryospheric processes and water resources becomes essential for effective water resource management, sustainable development, and disaster preparedness for the communities that rely on this awe-inspiring landscape for their livelihoods and well-being (Rashid, 2013).

3.2 Datasets

Table 3.1 showing the list of datasets used to conduct this study.

3.2.1 Daily streamflow data:

Daily streamflow data was required to be used as an input in model for calibration and further validation purposes. This data was collected from the Water and Power Development Authority's (WAPDA) project of surface water hydrology.

3.2.2 Weather Data:

As the study area has diverse topography and scarcely gauged with respect to its area so that we choose gridded dataset for temperature and precipitation.

The ERA5 atmospheric reanalysis, which covers the period from January 1940 to the present, is the fifth generation of the ECMWF. The Copernicus Climate Change Service (C3S) at ECMWF creates ERA5. Many atmospheric, land, and oceanic climate variables are provided hourly estimates by ERA5 (<https://www.ecmwf.int/>). This data is freely available for public at (<https://cds.climate.copernicus.eu/>)

3.2.3 Climate Projections:

To model prospective hydrological conditions, we employed shared Socioeconomic Pathway (SSP) accessible through CMIP6 data repository. This catalog entry offers data on daily and monthly global climate projections from a wide range of experiments, models, and time periods computed as part of the Coupled Model Intercomparison Project's (CMIP6) sixth phase. Climate projection experiments following the combined pathways of Shared Socioeconomic Pathway (SSP) and Representative Concentration Pathway (RCP). The SSP scenarios provide different pathways of the future climate forcing. The period covered is typically 2015-2100. This data is freely available for public at (<https://cds.climate.copernicus.eu/>).

Table 3.1. Showing the list of datasets used to conduct this study.

Data type	Data source	Scale	Description
DEM	ASTER GDEM (30m)	30 x 30 m	ASTER GDEM of the USGS
Snow Cover	MOD10A1 from nsidc.org	500 x 500 m	MODIS daily snow cover data
Weather Data	ERA5 data	Daily at hourly basis	Downloaded from Climate data store Copernicus
Climate Projections	CMIP6	Daily	Historical (1985-2014) Future (2015-2099)
Streamflow Data	WAPDA	Daily basis	To calibrate and validate the model

3.2.4 Digital Elevation model (ASTER GDEM):

A global digital elevation model (DEM) of land areas on Earth is provided by the Terra Advanced Spaceborne Thermal Emission and Reflection Radiometer (ASTER) Global Digital Elevation Model (GDEM) Version 3 (ASTGTM) at a spatial resolution of 1 arc second (roughly 30-meter horizontal posting at the equator) (Figure 3.2.). The National Aeronautics and Space Administration (NASA) and Japan's Ministry of Economy, Trade, and Industry (METI) have worked together to develop the ASTER GDEM data products. The ASTER GDEM's coverage area stretches from 83° North to 83° South. Each tile is made available through NASA Earthdata Search in Cloud Optimized GeoTIFF (COG) and NetCDF4 format as well as the LP DAAC Data Pool in standard GeoTIFF format. The 1984 World Geodetic System (WGS84)/1996 Earth Gravitational Model (EGM96) geoid is used to project data. At least 0.01% of the 22,912 tiles in the collection have land area (nsidc.org).

The data was used in this study to define the catchments for the Gilgit and Hunza rivers and to extract physical characteristics like elevation, slope, and catchment area. Understanding the physiography of the Gilgit and Hunza region requires elevation data. Different elevation zones and an area elevation curve are created using elevation data. The zonal mean hypsometric elevation and zonation of the aforementioned rivers' catchments are both calculated using this curve.

3.2.5 Snow cover data:

This data set contains daily, gridded snow cover and albedo derived from radiance data acquired by the Moderate Resolution Imaging Spectroradiometer (MODIS) on board the Terra satellite. Snow cover is identified using the Normalized Difference Snow Index (NDSI) and a series of

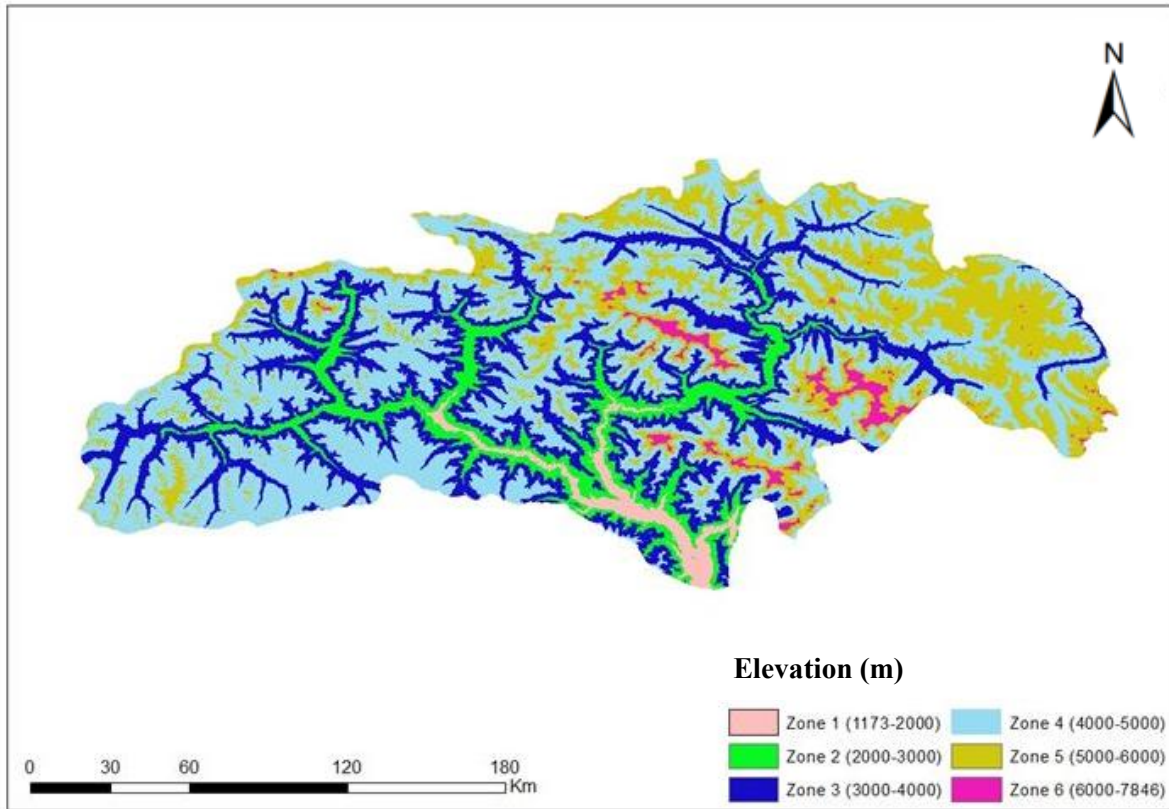


Figure 3.2. DEM showing area elevation zones.

screens designed to alleviate errors and flag uncertain snow cover detections (<https://nsidc.org/>). A large number of previous researches (Azmat et al., 2018; (Tahir et al., 2011) (Zhang et al., 2014); (Azmat et al., 2019); (Muhammad et al., 2017)) have used Modis snow cover products and found it useful for snowmelt runoff modelling. UIB river runoff can be accurately predicted using MODIS snow cover as an input data to the hydrological runoff model, according to research on the impact of SCA on the river (Immerzeel et al., 2009). The possible values for NDSI snow cover are given in Table 3.2.

3.3 Methodology

3.3.1 Hydro Modelling:

There are several appealing aspects to the idea of using regional hydrologic models to evaluate the effects of climatic change. First, there is no shortage of models that have been tested under various climatic and physiographic conditions, as well as models that are designed for use at different spatial scales and with different dominant process representations. This enables flexibility in determining and selecting the most suitable method to evaluate any region. Second, hydrologic models can be modified to fit the properties of the data that are currently available. The study purpose, model, and data accessibility have been the main determinants in choosing a model for a given case study among other variables. (Xu et al., 1999)

All models do, in fact, have applications in various fields. However, the simpler models, which have a smaller range of applications, can deliver adequate results at a significantly lower cost, provided that the objective function is appropriate. The more complex models, which have a wider range of applications, may be expected to deliver adequate results. Simple and physically based distributed-parameter models can be classified according to their intended uses as well as their degree of sophistication, which can range from low to high. The equivalent of selecting a suitable

model is deciding when simple models can be used and when complex models must be used. (Xu et al., 1999)

3.3.2 Snowmelt Runoff Model (SRM)

To simulate and predict daily streamflow in mountain basins where snowmelt is a significant runoff factor, the Snowmelt-Runoff Model (SRM) was created. Most recently, it has been used to assess how a changing climate will affect seasonal snow cover and runoff. (Martinec, 1975) created SRM in little European basins. SRM has been used in ever-larger basins as a result of the development of satellite-based remote sensing of snow cover. (Martinec et al 1983)

Over the past decades, hydrologists have been actively exploring viable methods to model snowmelt and its influence on runoff. As a result, two primary approaches, namely the energy-balance method and the degree-day method, have been introduced. (Zhang et al., 2014) The energy-balance approach emerges as a highly comprehensive technique, offering a holistic means to model and evaluate surface flow through the intricate energy exchange among snow, soil, and air. Nonetheless, its extensive data requirements pose a limitation, making its application unfeasible in basins with inadequate data availability (Abudu et al. 2016). Degree-day base models are more practical than energy-balance models, especially in basins with little available data. The most important factor in this process, according to some researchers' studies, is temperature. Models using the degree-day approach are well known for being straightforward and have been successfully used in several studies. (Nourani et al 2021)

Snowmelt runoff model (SRM) is a degree-day-based model, designed to simulate the impact of snowmelt, where it is a significant proportion of the water supply on watershed daily runoff (Martinec, 1975).

3.3.3 Structure of Model:

By adding estimations of snowmelt and rainfall runoff, which are then combined with recession flow, the Snow melt Runoff Model (SRM) computes the catchment's daily runoff data, the model is described by following Equation.

$$Q_{n+1} = [C_s a_n (T_n + \Delta T_n) S_n + C_r P_n] \times \frac{A \times 10^4}{86,400} (1 - k_{n+1}) + Q_n K_{n+1} \quad (1)$$

In this equation

Q = Discharge per day measured in [m³s⁻¹]

C = C_s and C_r are runoff coefficients for snow and rain respectively

a = degree-day factor [cm °C⁻¹ d⁻¹]

T = number of degree days [°Cd]

S = the ratio of the total area that is covered in snow

P = the precipitation that results in runoff [cm]

A = Total area of catchments [km²]

K = recession coefficient

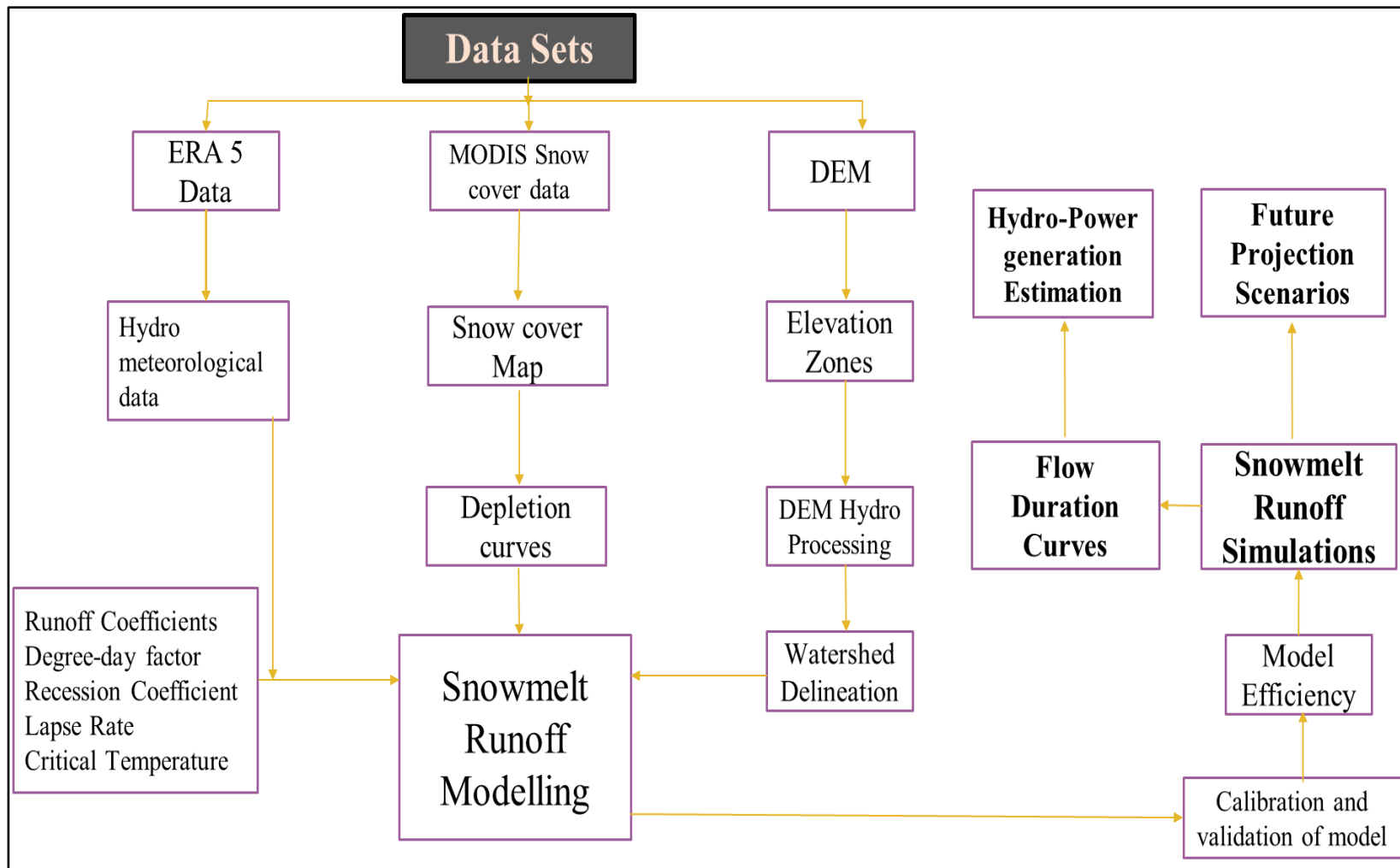


Figure 3.3. Showing methodology flowchart.

RESULTS AND DISCUSSION

4.1 Analysis of snow cover area

The seasonal variations of snowfall and melt within the Gilgit and Hunza River basin are valuable insights gained from the analysis of the mean monthly snow cover area images. Figure (3.1) shows the observed patterns demonstrate how the hydrological regime is affected by the snow cover's dynamic nature.

4.1.1 Winter Months (December - March):

Most of the region's landscape is covered in snow during the winter, with more than 80% of it covered. The coldest months of the year, January, and February are when snowfall is at its highest. The region's water resources benefit greatly from the extensive snow cover during the winter, which stores water in the form of snowpack that later contributes to spring runoff.

4.1.2 Transition Period (April - May):

Snow cover area is clearly decreasing as spring approaches. The snowmelt phase begins in April, and by May, the area covered by snow has decreased by 20–30%. This decrease in snow cover signals the beginning of snow melt and the changeover from a hydrological regime dominated by snow to one that is triggered by rainfall and warmer temps.

4.1.3 Warmer Months (June - October):

Snow cover significantly decreases from June to October, with higher elevations only having sporadic patches of snow. When compared to the winter months, the snow cover drops the fastest

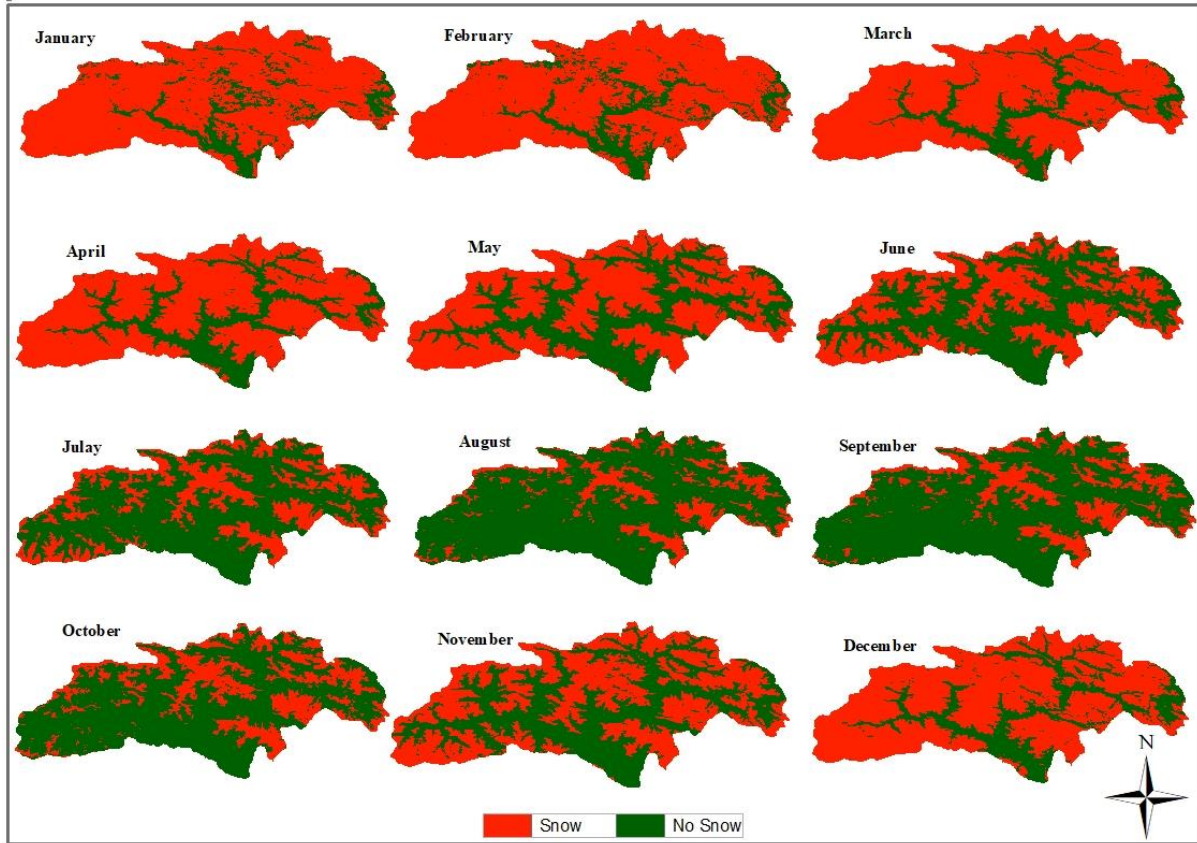


Figure 4.1. Change in Snow cover area over Gilgit and Hunza river basin during each month of a year.

in the months of June and July, by up to 70–80%. Snowmelt has been accelerated by rising temperatures and solar radiation, which are the main causes of this reduction.

4.1.4 Late Autumn (November):

The snow cover area continues to shrink as the year moves into late autumn, approaching its minimum extent. By November, the landscape had largely changed from being covered in snow to being snow-free, preparing it for the approaching winter deposition season.

4.1.5 Zonal Snow cover analysis.

In simple terms, the Figure (zonal snow graph) tells interesting results about how elevation zones respond to fluctuations in the seasons, providing insightful information about the complicated nature of snow cover and its impact on the hydrological processes in the study area. These discoveries are of utmost importance for streamlining water resource distribution and supervision plans, particularly considering climate change. The line graph clearly illustrates variations in snow cover patterns over time for three different elevation zones. Zone 6, which is notable, has the longest-lasting and uniform snow cover over the year, with the winter months boasting an impressive snow cover percentage of over 95%. This pattern can be attributed to the enhanced snowpack preservation during colder seasons caused by the elevated altitude.

Zone 4 exhibits a startlingly different reaction. As the warmer months arrive, a noticeable decline can be observed, with percentages falling to just 20%. This extreme depletion shows how quickly rising temperatures and more solar radiation influence lower-altitude snowpack. This dynamic phenomenon emphasizes this zone's susceptibility to seasonal changes and the area's reliance on meltwater from higher elevations for sustained water resources during the dry months. Zone 5 exhibits an intermediate snow cover behavior due to its intermediate elevation range which is 5000 to 6000 meters. During the transition to summer, its snow cover gradually decreases but

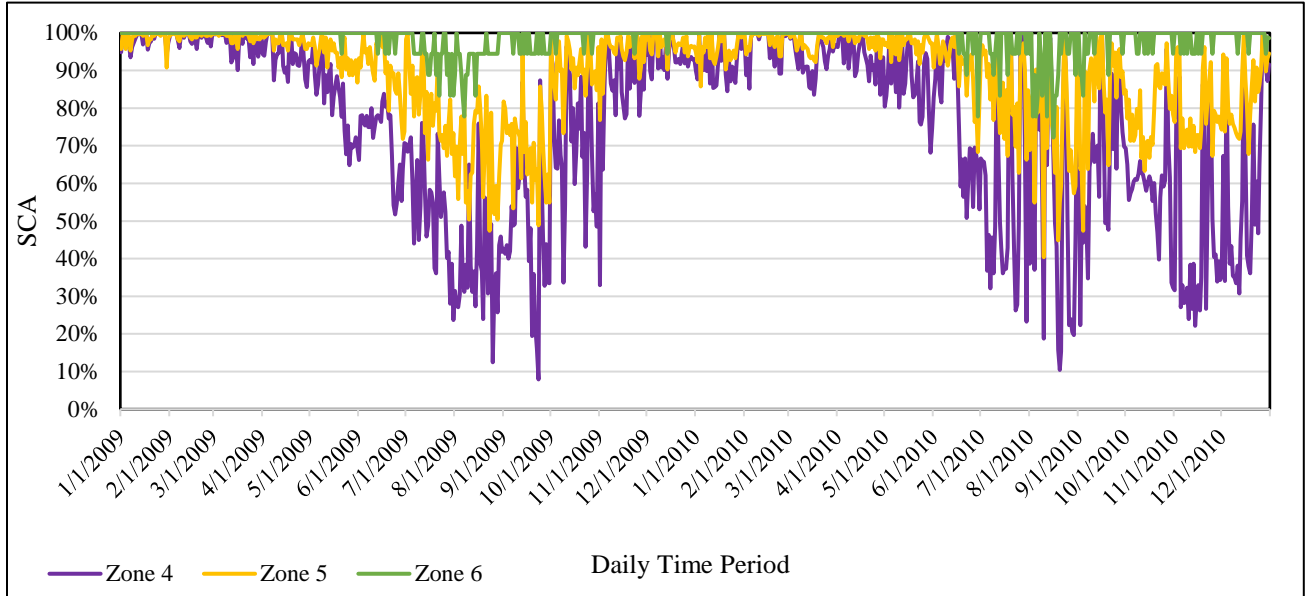


Figure 4.2. Zone wise trends SCA for years 2009-10.

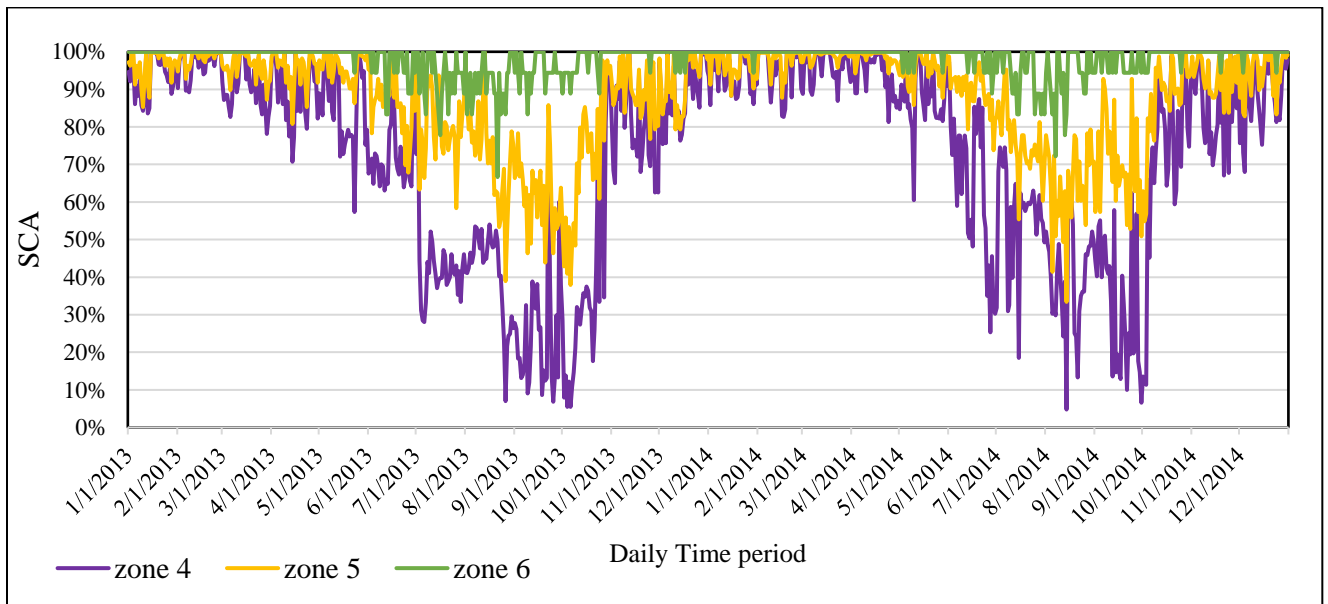


Figure 4.3. Zone wise trends SCA for years 2013-14.

still retains a greater extent than Zone 4. The complex interactions between elevation, temperature, and snow cover are highlighted by these findings, underscoring the significance of elevation-dependent streamflow simulations and effective resource management approaches designed to each zone's particular exposure to snowmelt fluctuations.

4.2 Analysis of Runoff Simulations

The resulting graphs Figure (4.4) and Figure (4.5) show a positive correlation between simulated and observed stream flows. Its reliability as a tool for modeling and comprehending hydrological dynamics is strengthened by the model's ability to replicate observed runoff patterns, particularly the stated peak discharges during summer. Although acknowledged, the slight variations in runoff volumes do not diminish the model's overall effectiveness in capturing the essence of the produced runoff and its variation with the seasons.

The snowmelt runoff model's output graphs provide a thorough representation of the model's effectiveness in modeling runoff during the calibration stage between 2009 and 2010. The comparison of measured and computed runoff provides an understanding of the model's precision and ability to accurately represent real-world hydrological processes in addition to serving as a visual validation of the model's effectiveness.

The model performs satisfactorily across both calibration years, with only a slight discrepancy between the estimated and measured runoff volumes. With a volume difference of just 2.86% in 2009, the model and measured runoff show a commendable similarity. The model also shows a difference of 1.09% in 2010, further demonstrating its reliability in obtaining runoff behavior.

Although the minor disparities in the levels of runoff may cause some concern, it's important to place these variations in the context of the larger hydrological complexities. Such variations can

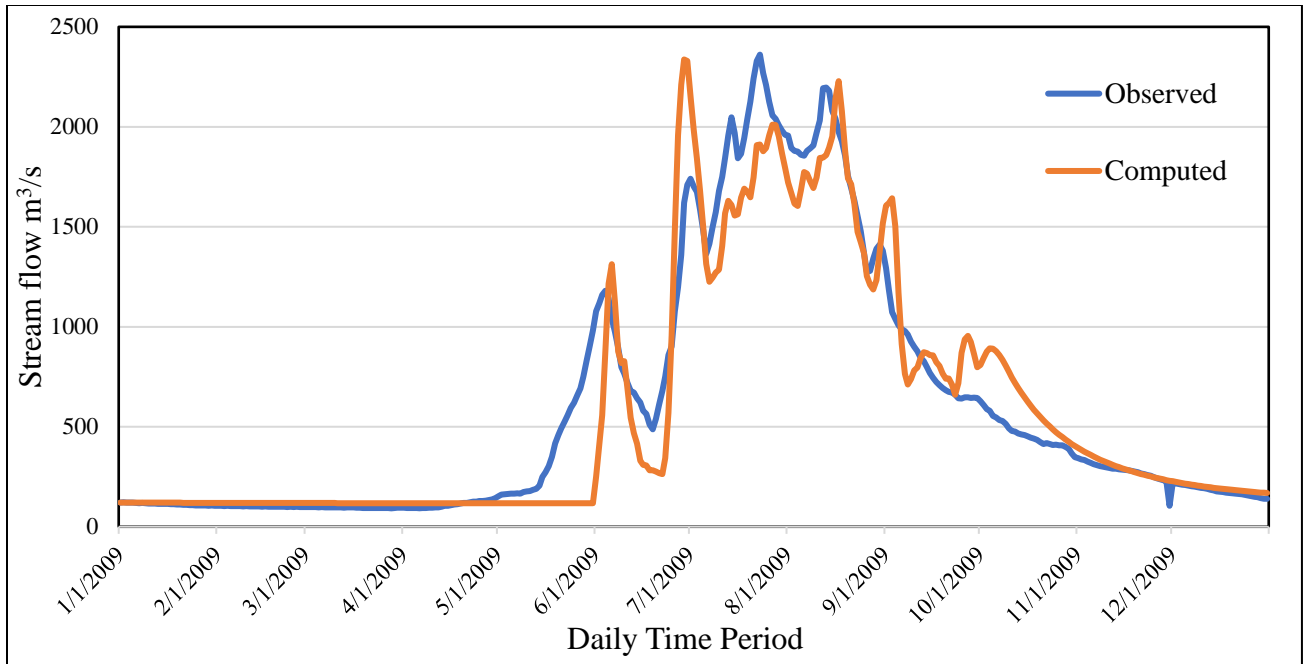


Figure 4.4. Measured vs Computed runoff for calibration period 2009.

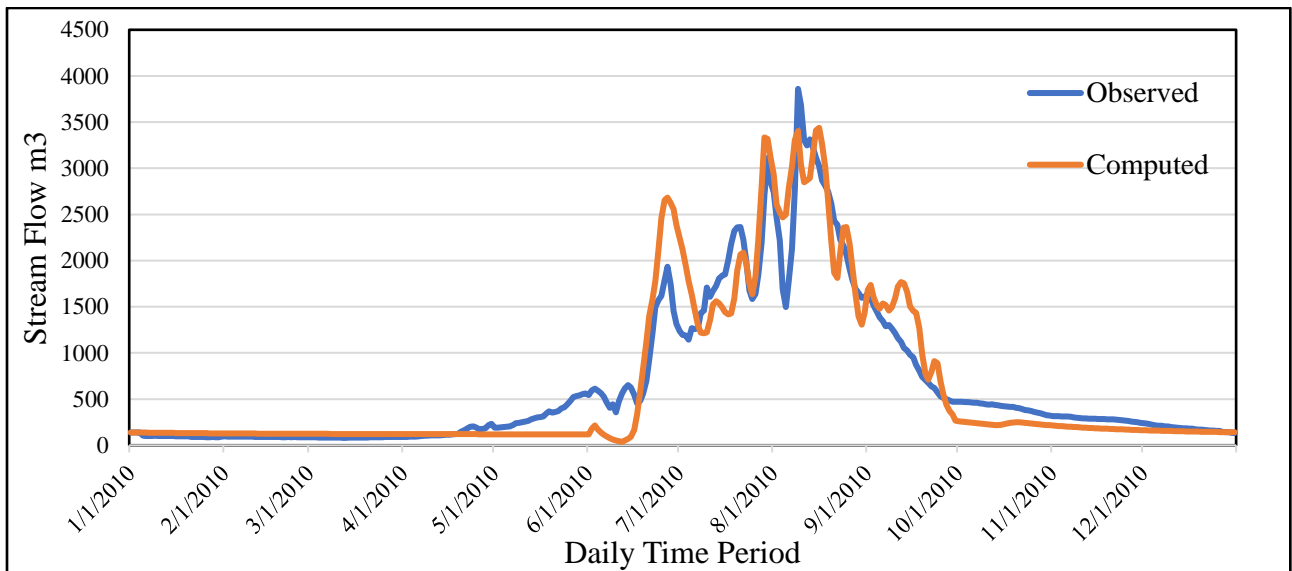


Figure 4.5. Measured vs Computed runoff for calibration period 2010.

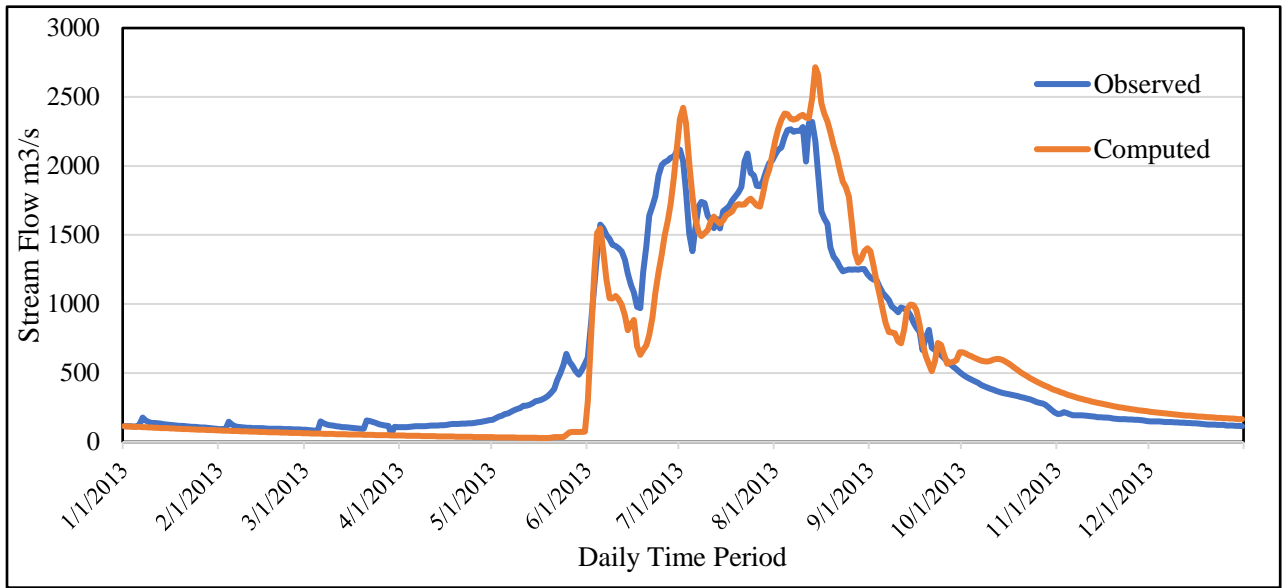


Figure 4.6. Measured vs Computed runoff for validation period 2013.

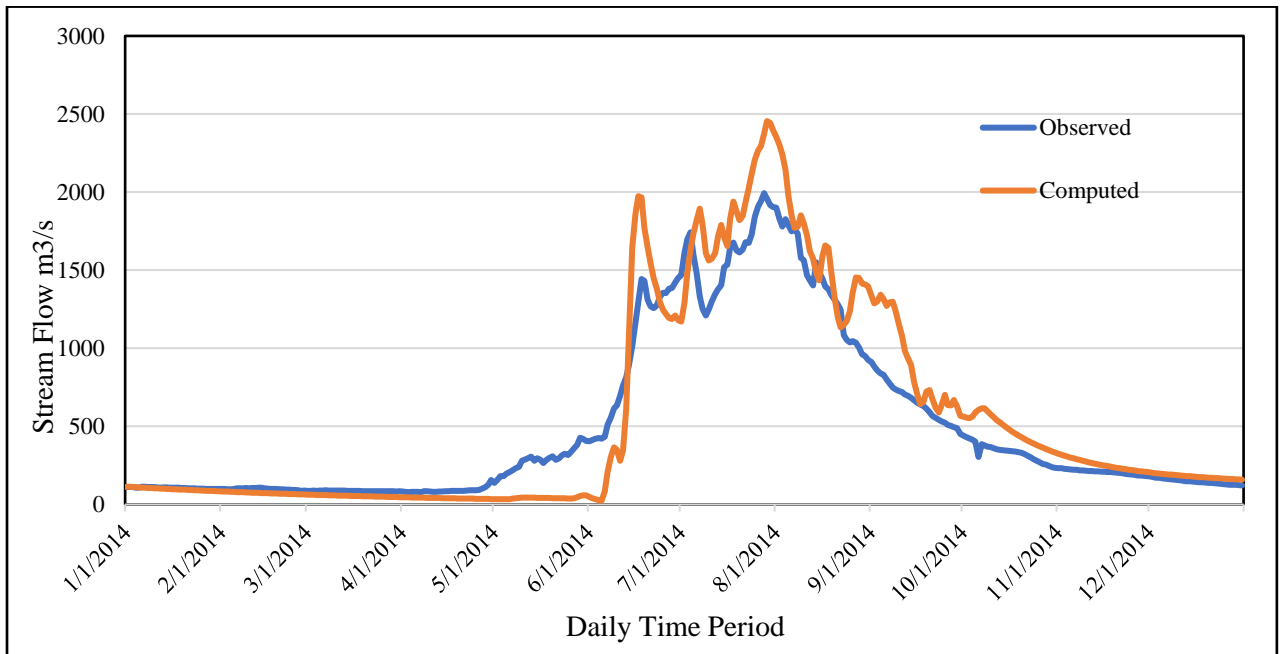


Figure 4.7. Measured vs Computed runoff for validation period 2014.

Table 4.1. Showing zone wise parameter values.

Parameters		Zone 1	Zone 2	Zone 3	Zone 4	Zone 5	Zone 6
Lapse rate (°C/100m)		0.5	0.55	0.64	0.69	0.74	0.76
T_{crit} (°C)		1.3	1.3	1.3	1.3	1.3	1.3
DDF (cm°C⁻¹d⁻¹)	Sep - April	0.53	0.58	0.64	0.68	0.73	0.8
	May - August	0.48	0.53	0.59	0.65	0.7	0.75
Lag time (hrs)		7	10	13	15	17	19
Cs	Sep - April	0	0.22	0.33	0.38	0.42	0.45
	May - August	0	0.3	0.38	0.46	0.49	0.51
Cr	Sep - April	0.6	0.37	0.35	0.22	0.09	0
	May - August	0.42	0.5	0.42	0.32	0.15	0
RCA	Sep - April	1	1	1	0	0	0
	May - August	1	1	1	1	0	0
Xc	Sep - April	1.1	1.1	1.1	1.1	1.1	1.1
	May - August	0.9	0.9	0.9	0.9	0.9	0.9
Yc	Sep - April	0.02	0.02	0.02	0.02	0.02	0.02
	May - August	0.02	0.02	0.02	0.02	0.02	0.02

be caused by variables like spatial heterogeneity, uncertainties in the input data, and the innate variability of natural systems. Nevertheless, the model's general consistency between simulated and observed runoff volumes highlights its usefulness as a predictive tool and strengthens the model's credibility. Hydrological intuition predicts that the heat of the summer will produce the highest discharges because of increased streamflow caused by increased snowmelt during this time. This finding highlights the model's potential value for well-informed decision-making in handling water resources, predicting floods, and ecosystem preservation in addition to confirming the model's competence.

4.3 Assessment of Model Efficiency Tests

Through a series of efficiency tests, the performance of the model is evaluated, and this gives us an extensive knowledge of its forecasting abilities. In the context of this study, metrics such as the coefficient of determination (R^2), Nash-Sutcliffe Efficiency (NSE), and the volume differences between computed and measured runoff are used to assess the model's efficacy. (Table 4.2.)

4.3.1 Coefficient of determination R^2 :

The calibration period's R^2 values of 0.89 and 0.87, as well as the validation period's R^2 values of 0.88 and 0.85, show that the simulated and observed runoff have a strong linear relationship. Table (3.1) These numbers indicate that the model can account for between 89% and 87% (calibration) and 88% to 85% (validation) of the observed runoff variability. The model's capacity to capture broad trends and variations in runoff is highlighted by its high R^2 values, which points to an accurate depiction of the underlying hydrology.

Table 4.2. Model efficiency results

Efficiency Parameters	Calibration		Validation	
	2009	2010	2013	2014
R ²	0.89	0.87	0.88	0.85
Dv	2.86%	1.09%	2.91%	8.97%
NSE	0.893	0.875	0.883	0.857

4.3.2 Volume Difference in Percentage (Dv%)

The small volume differences between computed and measured runoff — 2.86% and 1.09% for calibration, and 2.91% and 8.97% for validation — show a promising correlation between model predictions and empirical data. The calibration proficiency of the model is demonstrated by the relatively small volume differences during calibration and the close agreement between the observed and simulated runoff values. The model performs satisfactorily in predicting runoff volumes across the various datasets, even though slightly larger deviations are observed during validation. They nevertheless remain within reasonable bounds.

4.3.3 Nash-Sutcliffe efficiency Test (NSE)

The NSE values for calibration and validation period were 0.893 and 0.875, and 0.883 and 0.857, respectively, illustrate the model's ability to accurately represent the observed runoff variability. Greater agreement between the modeled and observed values is indicated by NSE values that are nearer to 1. The model's predictability and its potential for practical applications are strengthened by the achieved NSE values, which show a significant agreement between the model's predictions and the actual runoff.

These efficiency measurements confirm the model's ability to accurately simulate runoff dynamics when taken as a whole. The capability to compute runoff variations and trends is highlighted by the high R^2 values and NSE scores, which support its validity as a hydrological modeling tool. The slight volume differences, even within validation, are well within the range of acceptance further demonstrating the robustness of the model. Such performance guarantees are essential for enhancing the model's usefulness in informing flood forecasting, water resource management, and the formulation of decisions.

4.4 Comparison of Streamflow with Trends in SCA

The Figure (3.6) beautifully depicts how the amount of snow cover changes over three elevation zones and its relationship with the stream flows. Snowmelt has begun when there is a noticeable decrease in the snow cover area in summer months throughout all elevation zones. The correlation between reduced SCA and increased streamflow emphasizes the crucial contribution of snowmelt to boosting streamflow levels. The melt process is accelerated during the summer because of the increased exposure to sunlight and higher temperatures. The resulting meltwater percolates into nearby waterways as the snowpack decreases, increasing streamflow. This observed increase in river runoff is a direct result of the accelerated snowmelt, a significant hydrological process that boosts water availability in the area.

4.5 Sensitivity analysis

The sensitivity analysis of model was performed manually by increasing and decreasing parameters 10 to 20% one by one. The model's performance was iteratively improved to increase the degree of agreement between simulated and measured runoff by incrementally changing parameter values. This manual adjustment procedure was designed to correct any errors or biases in the model's initial parameterization, improving the model's capacity to accurately represent the subtleties of the hydrological system under investigation.

The DDF and recession coefficients were found to be more sensitive in this process. Slightly change in these resulted in higher variations in model's results. The DDF values ranged between 0.53 to 0.8 in winter months while 0.48 to 0.75 for summer months. The values of Recession coefficients for x and y were 1.1 and 0.02 respectively.

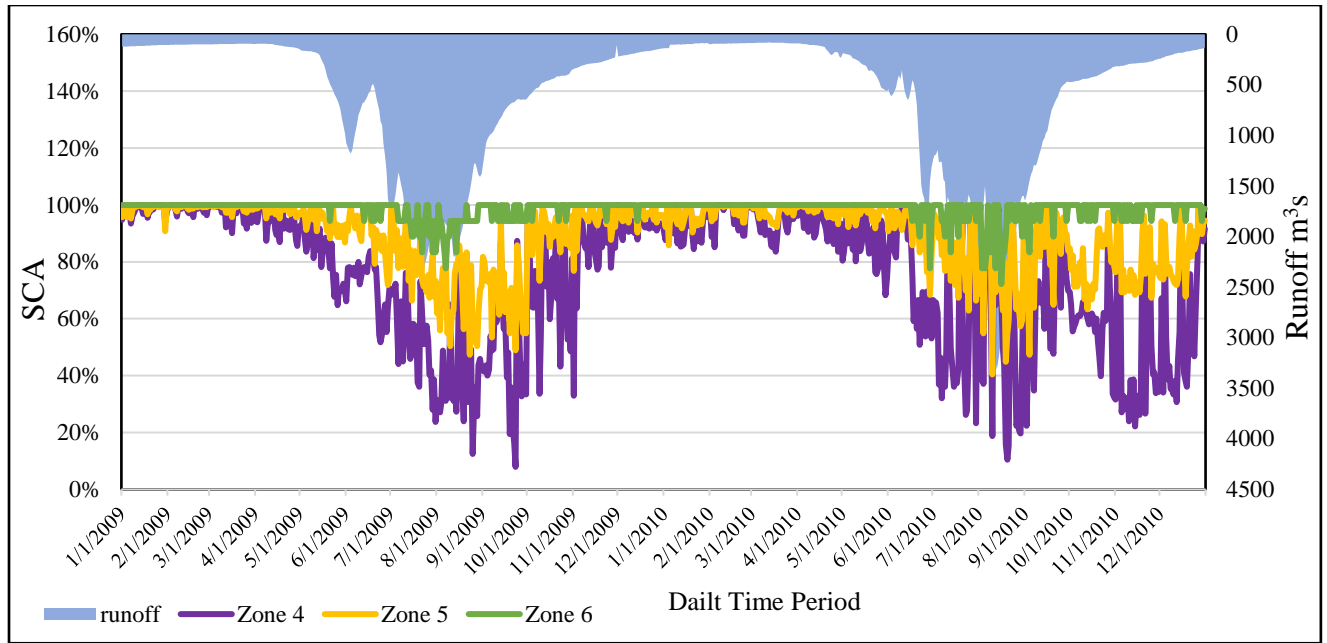


Figure 4.8. Comparison of streamflow with trends in SCA.

4.6 Analysis of future projections:

The complex relationship between temperature, precipitation, and hydrological responses is highlighted by the analysis of streamflow predictions within the context of future climatic projections using CMIP6 data for SSP2 and SSP5 scenarios. The trends in streamflow that are influenced by temperature highlight the need for extensive water management strategies that take potential temperature-induced changes into account. Even though the observed temperature increases range in magnitude from SSP2 to SSP5, they have a significant impact on predictions of streamflow. A slight increase in temperature values was observed in SSP2 scenario while a significant increase in minimum and maximum temperature values was found in SSP5 scenario which can cause a way more higher stream flows and it will have direct impact on streamflow patterns and the availability of water.

In contrast to temperature, there were small variations in precipitation values for future scenarios. As SRM is a degree day model the change in precipitation values might not affect the stream flows while a small variation in temperature can have direct impact of runoff volume.

4.7 Impact of Future Projections on Stream Flows

In Figure (4.15) streamflow trends show a significant trajectory of change that may portend hydrological shifts in the ensuing decades. For future climate change scenario SSP2-4.5 The model predicts a streamflow increase of 18% by 2030, with a calculated discharge (Q) of 674 m³/s. This increase highlights the impact of the scenario on hydrological processes and points to a significant change in water availability. The streamflow projection for the 2060s shows a more noticeable shift, with a 21% increase and a resulting discharge of 688 m³/s. The most notable change, however, occurs in the 2090s, when the streamflow is projected to reach a discharge of 822 m³/s,

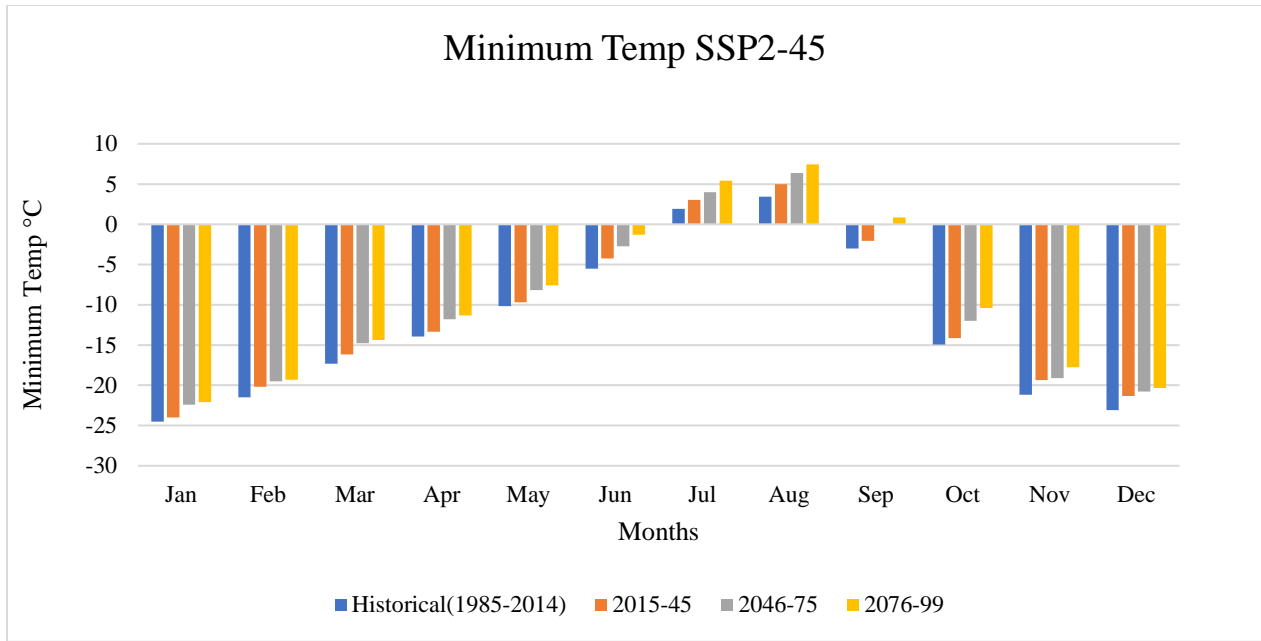


Figure 4.9. Future projections for change in minimum temperature under SSP2-45.

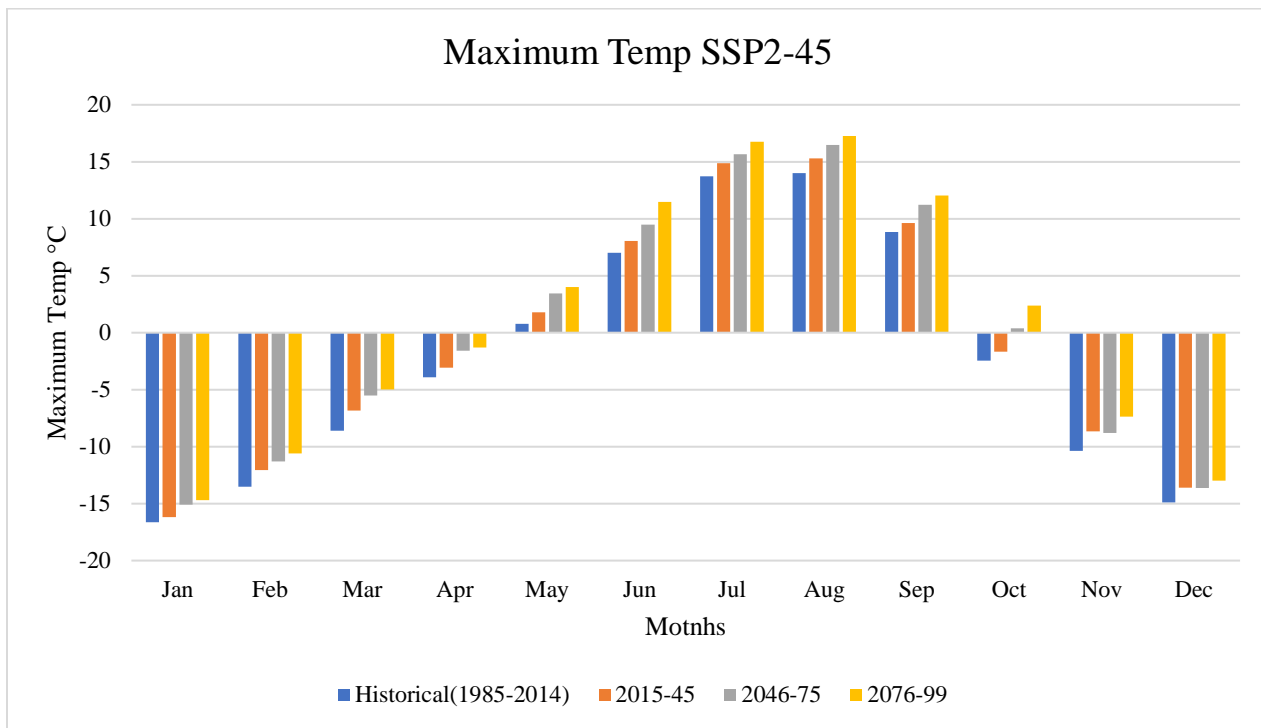


Figure 4.10. Future projections for change in maximum temperature under SSP2-45.

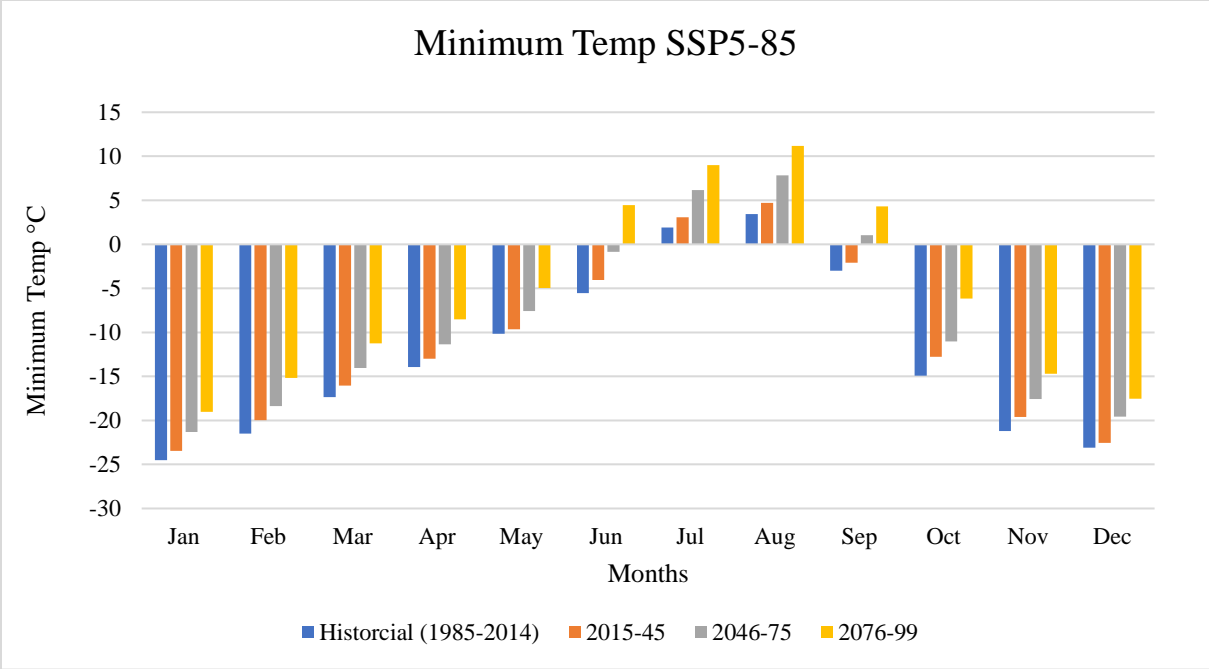


Figure 4.11. Future projections for change in minimum temperature under SSP5-8.5.

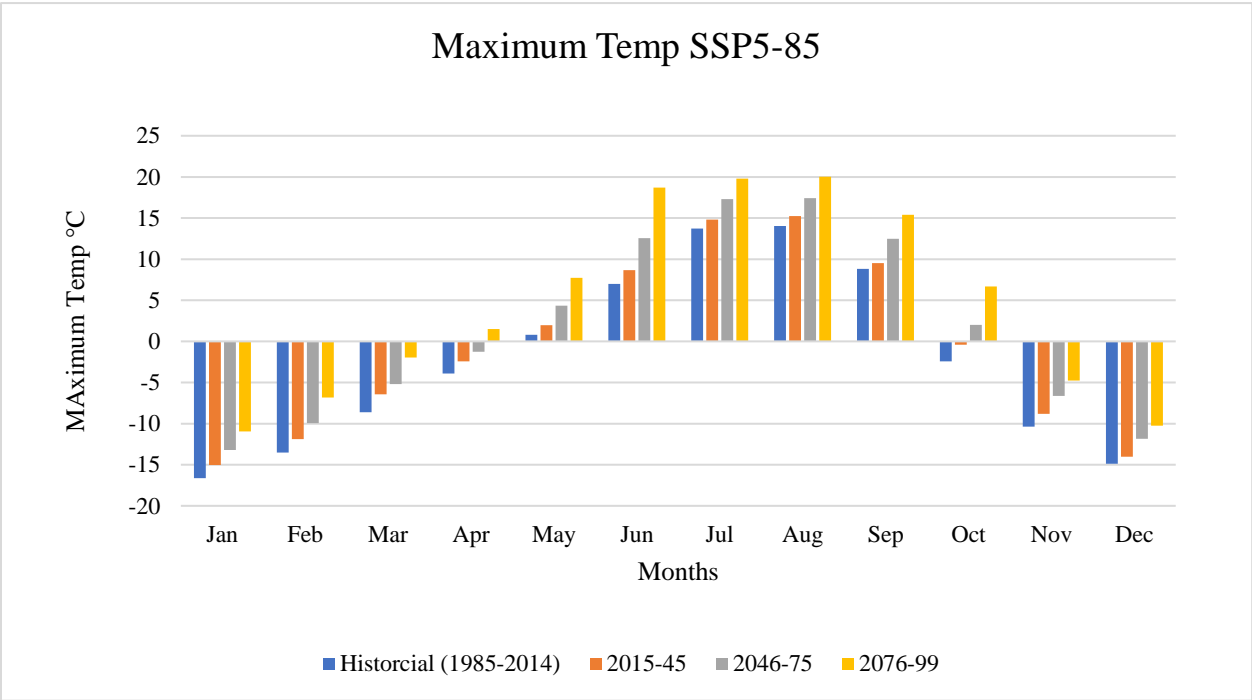


Figure 4.12. Future projections for change in maximum temperature under SSP5-8.5.

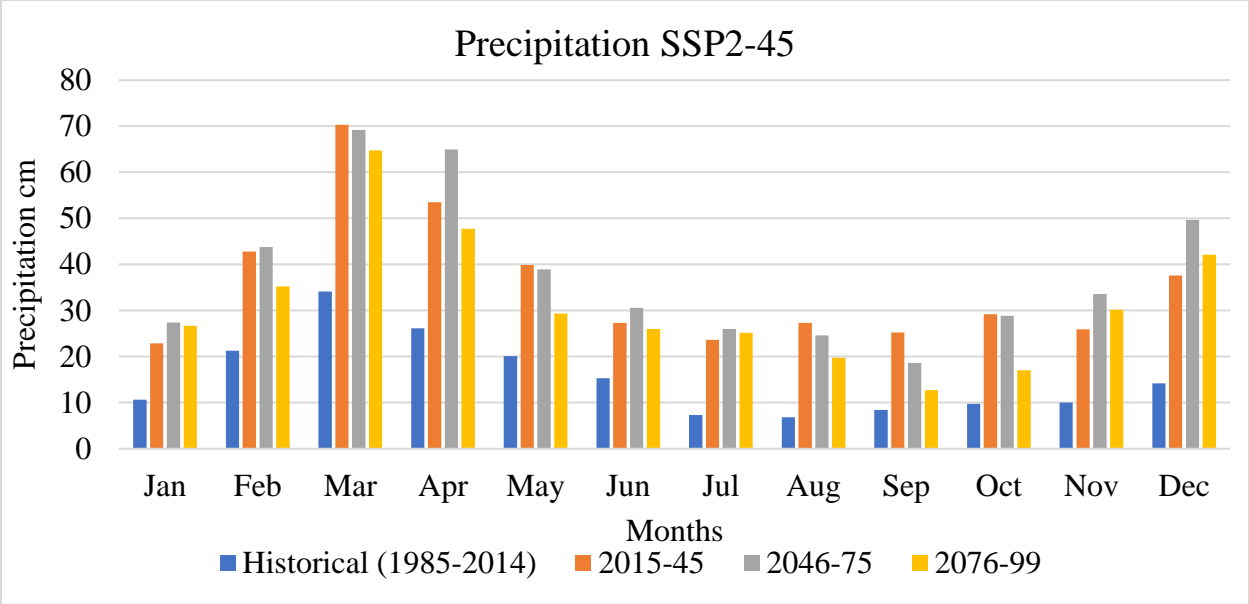


Figure 4.13. Future projections for change in precipitation under SSP2-4.5.

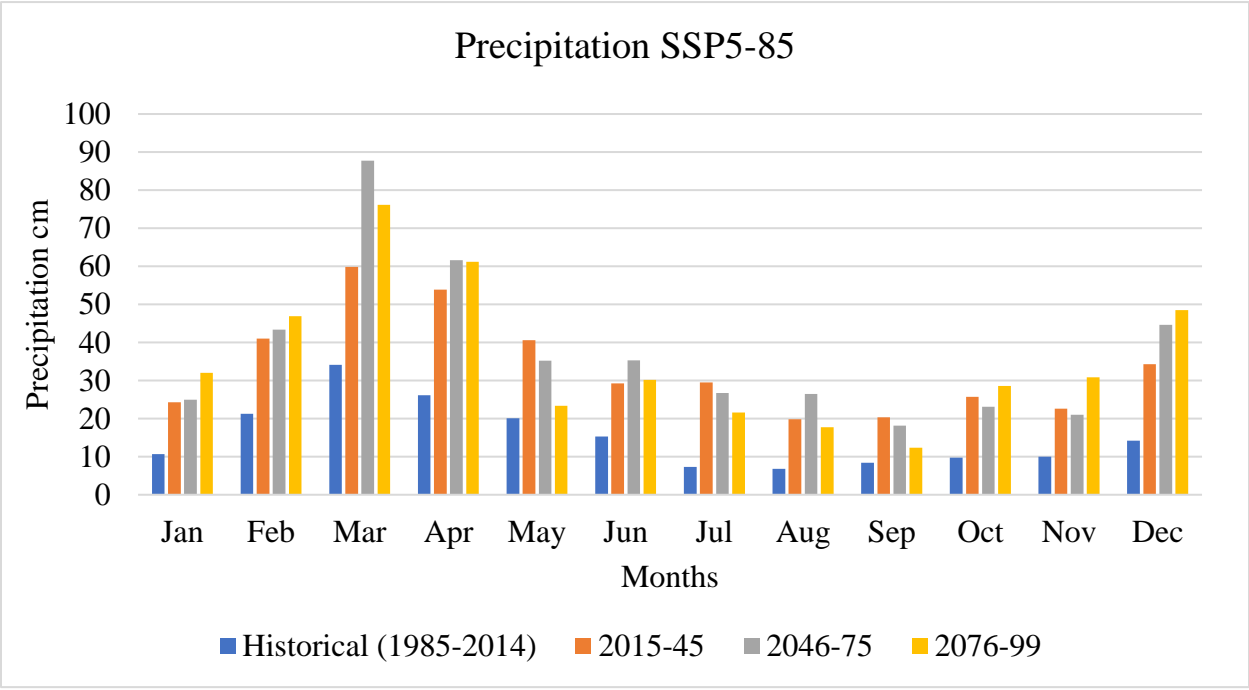


Figure 4.14. Future projections for change in precipitation under SSP5-8.5.

reflecting a significant 44% increase from the current average daily streamflow. Table (2) This surge denotes a significant alteration in the area's hydrological dynamics, which may be related to a confluence of socioeconomic and climatic factors included in the SSP2 scenario.

The Figure (4.16) showing projected stream flows in the future under the SSP5-8.5 scenario reveals a compelling story of hydrological changes over time. The streamflow (Q) is predicted to increase significantly by 12% in the 2030s and reach 642. This initial increase portends a more noticeable shift in the 2060s, when the streamflow significantly increases by 45%, reaching a peak flow rate of 827. The 2090s see the most notable change, which paints a clear picture of the changing hydrological landscape. Here, the streamflow is anticipated to reach 1175, which would represent a remarkable 105% increase over the current daily average stream flow.

4.7.1 Contribution of Snow melt on Stream Flows:

The future projections also show the contribution of only snowmelt in stream flows. Figure (4.17) shows how increase in temperature in future boosting up the snowmelt rate hence contributing higher stream flows in future. The graph of snowmelt contribution under climate change scenario SSP2-4.5 indicates the 7.5% increase in 2030's, 11% and 33% increase in runoff in 2060's and 2090's respectively.

Figure (4.18) represents the snow melt contribution in future river flows under climate change scenario SSP5-8.5. It illustrates a 2.4% increase in 2030's while 38% increase in 2060's with $Q = 788 \text{ m}^3/\text{s}$ and a significant increase 91% in flows of 2090's was observed which was $Q = 1092 \text{ m}^3/\text{s}$. The rising temperature in future predicts the higher water level in rivers which can cause numerous effects on activities associated with these rivers.

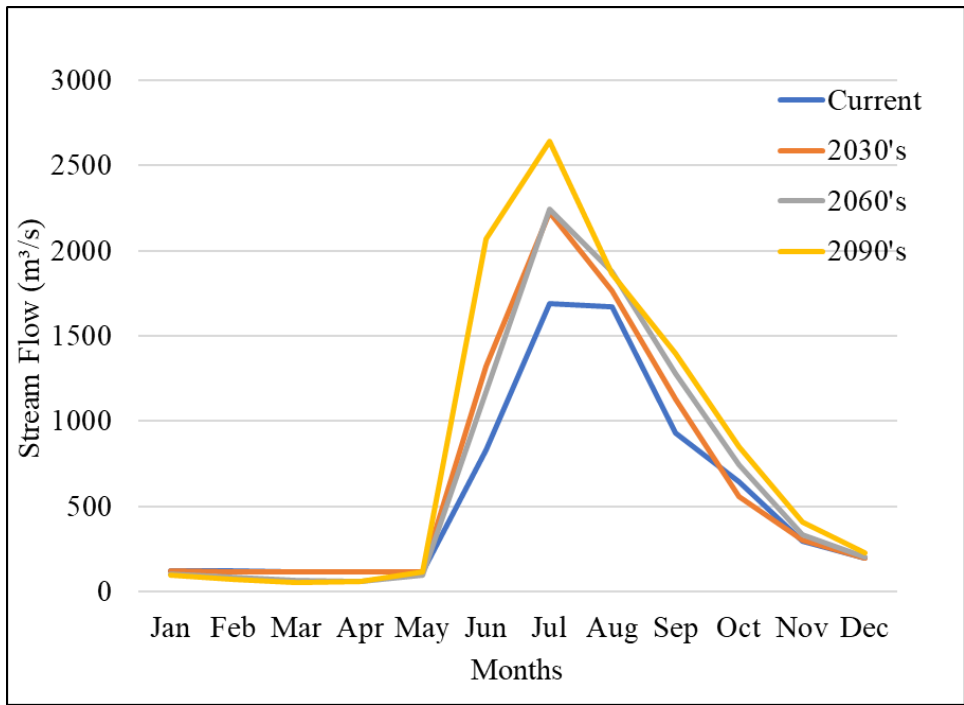


Figure 4.15. Projected streamflow under SSP2-4.5.

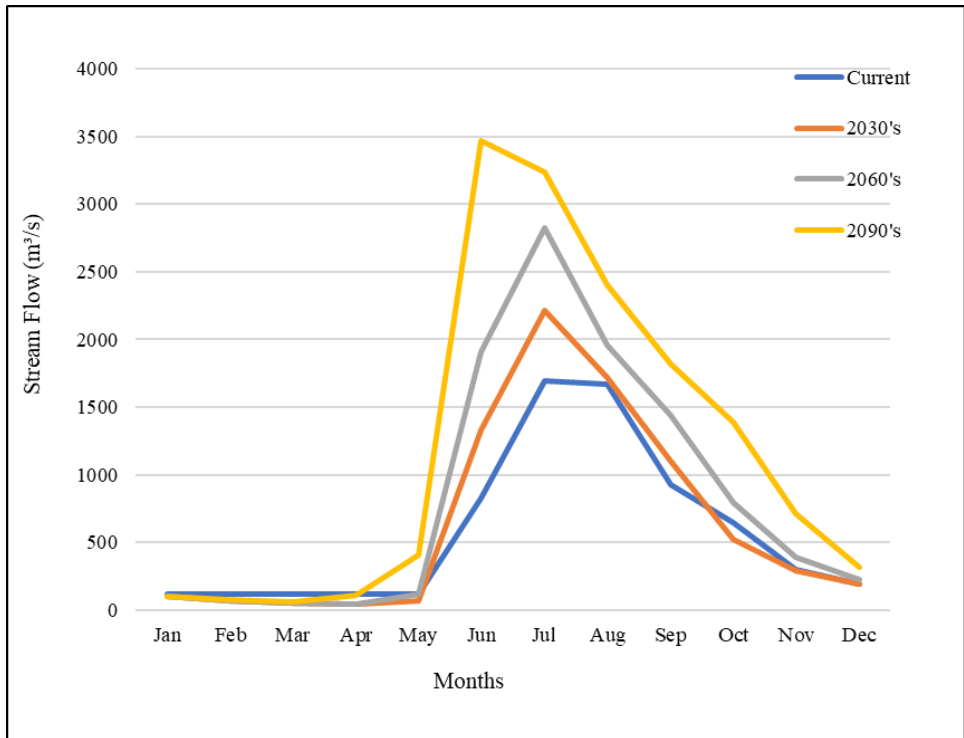


Figure 4.16. Projected streamflow under SSP5-8.5.

Table 4.3. Projected streamflow under current and future climate change scenarios.

Scenarios	Q (m³/s)	% Increase
Current Flow	571	-
For SSP2-4.5		
Increase in 2030's	674	18%
Increase in 2060's	688	21%
Increase in 2090's	822	44%
For SSP5-8.5		
Increase in 2030's	642	12%
Increase in 2060's	827	45%
Increase in 2090's	1175	105%

4.8 Flow Duration Curves

The flow duration curve Figure (4.19), an insightful illustration of streamflow variability, tells an engrossing story of anticipated hydrological changes under various hypotheses. The curve for Climate change scenario SSP2-4.5, which reflects the current hydrological conditions, shows a strong streamflow of $Q = 1612 \text{ m}^3/\text{s}$ in the current scenario. Looking ahead, the streamflow intensifies to $Q = 1841 \text{ m}^3/\text{s}$ at the 15% probability of exceeding it in the 2090s projection, indicating increased water availability in extreme events. The stream flows for the current period ($Q = 830 \text{ m}^3/\text{s}$), 2030s ($Q = 1084 \text{ m}^3/\text{s}$), 2060s ($Q = 1152 \text{ m}^3/\text{s}$), and 2090s ($Q = 1335 \text{ m}^3/\text{s}$) show an escalating pattern that reflects shifting hydrological dynamics over time. This trend continues at the 30% exceedance probability. Additionally, the current streamflow ($Q = 194 \text{ m}^3/\text{s}$) noticeably increases to $Q = 315 \text{ m}^3/\text{s}$ in the 2090s at the median exceedance probability of 50%, emphasizing the predicted increase in water availability. Collectively, these findings highlight how future scenarios may affect streamflow patterns, emphasizing the possibility of increased water volumes, especially in extreme and median events.

For climate change scenario SSP5-8.5 the projection from the present state to the 2090s depicts a significant change at the 15th percentile. Figure (4.20) In the current situation, the streamflow is $Q = 1612 \text{ m}^3/\text{s}$, meaning that it exceeds this value 15% of the time. But by the 2090s, there has been a noticeable change, and streamflow has increased to $Q = 3088 \text{ m}^3/\text{s}$ at the same percentile. This significant rise highlights the potential water volume amplification and the escalating hydrological dynamics under future conditions. The 30th percentile emphasizes these changes even more. Currently, $Q = 830 \text{ m}^3/\text{s}$, which shows that streamflow is occasionally exceeded (30%). Moving forward to the 2030s, the projection anticipates a moderate increase to $Q = 1000 \text{ m}^3/\text{s}$, which denotes a greater likelihood of flow occurrence. This pattern persists into the 2060s, when

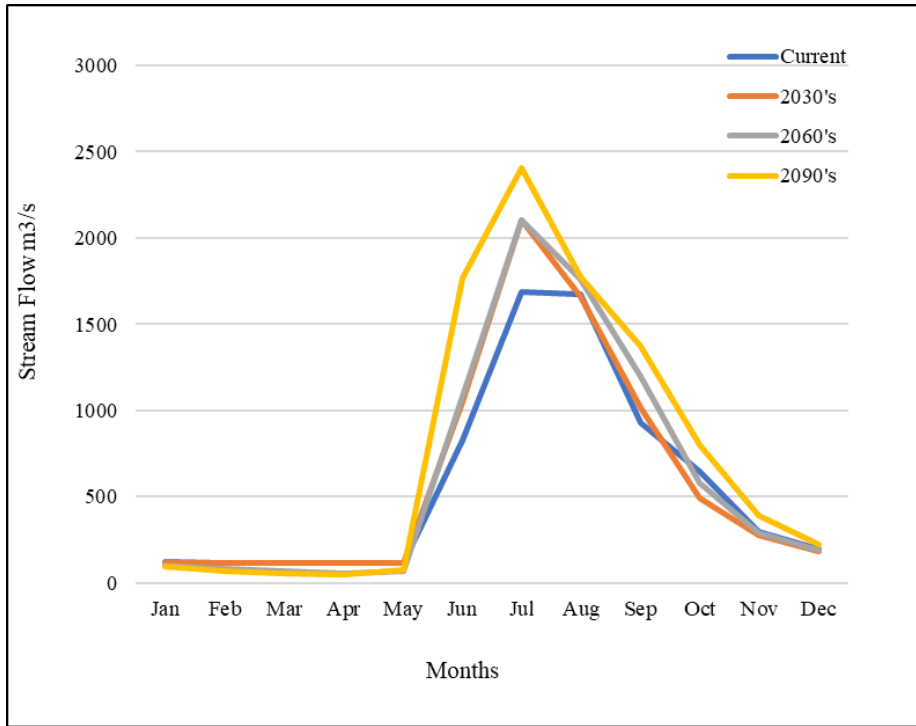


Figure 4.17. Projected streamflow by contribution of snow and glacier melt under climate change scenario SSP2-4.5.

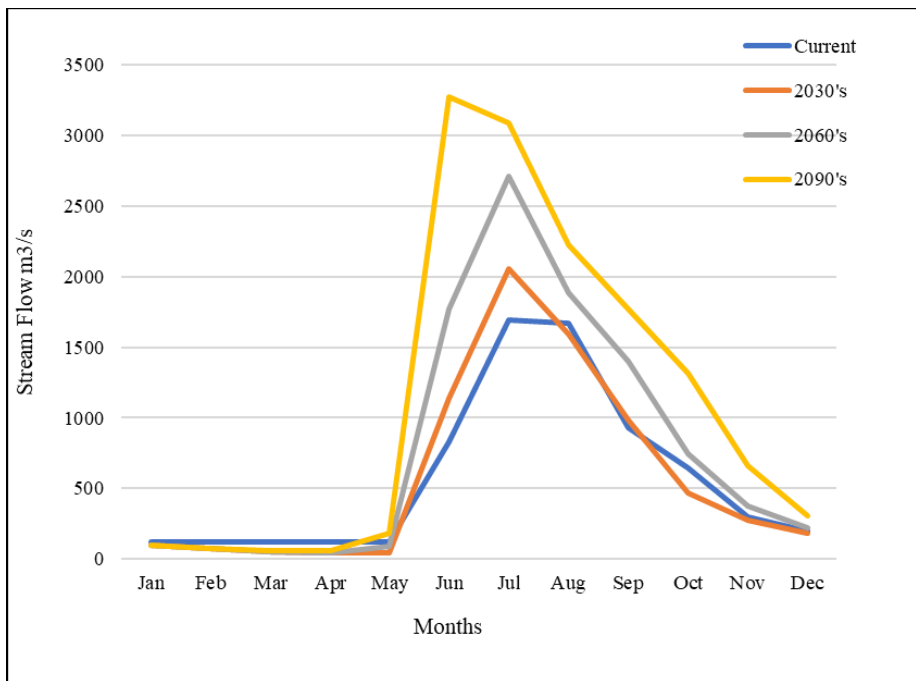


Figure 4.18. Projected streamflow by contribution of snow and glacier melt under climate change scenario SSP5-8.5.

Table 4.4. The contribution of snowmelt on projected streamflow under current and future climate change scenarios.

Scenarios	Q (m³/s)	% Increase
Current Flow	571	-
For SSP2-4.5		
Increase in 2030's	614	7.5%
Increase in 2060's	631	10.5%
Increase in 2090's	757	32.6%
For SSP5-8.5		
Increase in 2030's	584	2.4%
Increase in 2060's	788	38%
Increase in 2090's	1092	91%

$Q = 1333 \text{ m}^3/\text{s}$ denotes a significant increase in streamflow frequency. The hydrological landscape most dramatically changes in the 2090s, with $Q = 1837 \text{ m}^3/\text{s}$, showing a dramatic elevation. The contrast is equally noticeable at the median, or the 50th percentile. Streamflow is currently at $Q = 194 \text{ m}^3/\text{s}$. This rises to $Q = 211 \text{ m}^3/\text{s}$ in the 2030s, suggesting a gradual change. However, by the 2060s, the streamflow increases more significantly to $Q = 350 \text{ m}^3/\text{s}$, which represents a significant change from the current situation. The projection shows an even more pronounced shift by the 2090s, when streamflow soars to $Q = 606 \text{ m}^3/\text{s}$, clearly showing a significant shift in hydrological behavior.

4.9 Hydro-Power generation estimation:

An estimate of hydro power generation was calculated using the flow duration curve data. As the flow duration curve was drawn for current and future climate change scenarios. The comparison of current scenarios with SSP2-4.5 in Table (4.5) shows 14% increase in power generation by 2090's at 15% exceedance of time. While for 30% exceedance of time it shows 39% increase in power generation by 2060's and 61% increase in power production by 2090's.

Similarly, in the case of climate change scenario SSP5-8.5 an increase in power production was also observed under all future time periods. Table (4.6) For 15% exceedance of time an increase of 92% in power production in 2090's was calculated. For 30% exceedance in time 70% and 121% increase in power production was calculated for 2060's and 2090's respectively. And at 50% exceedance of time a significant increase of 80% and 212% was found for 2060's and 2090's respectively. This shows that projected increase in power production is highly dependent on higher river flows.

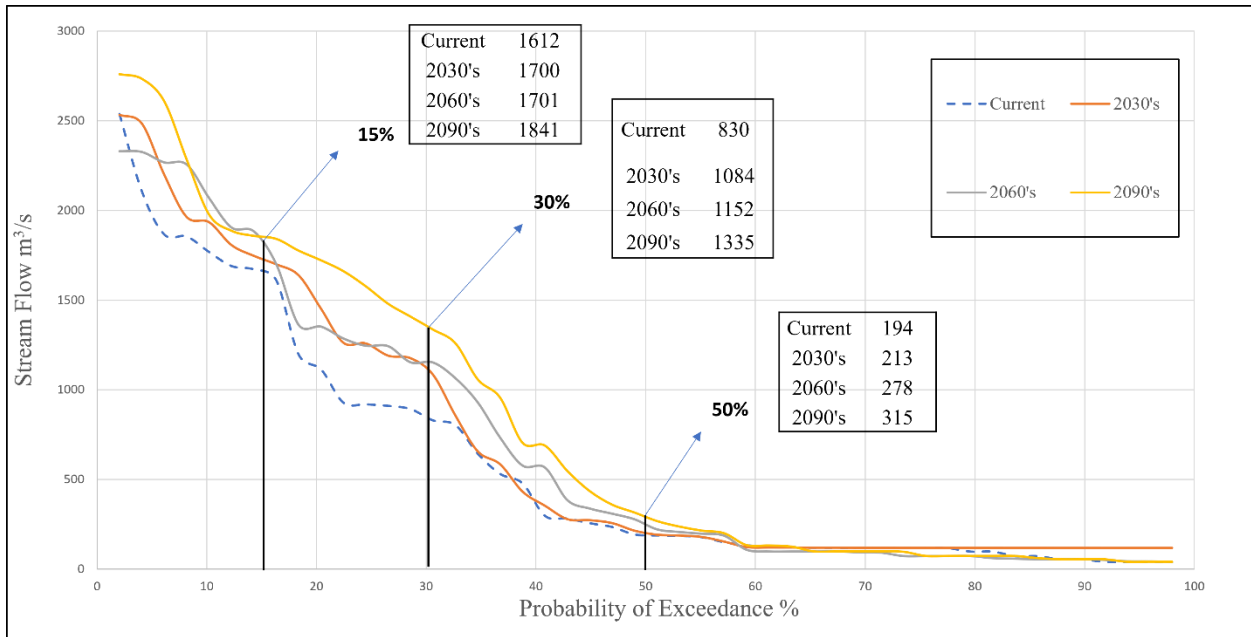


Figure 4.19. Flow duration curve for future stream flows under climate change scenarios SSP2-4.5.

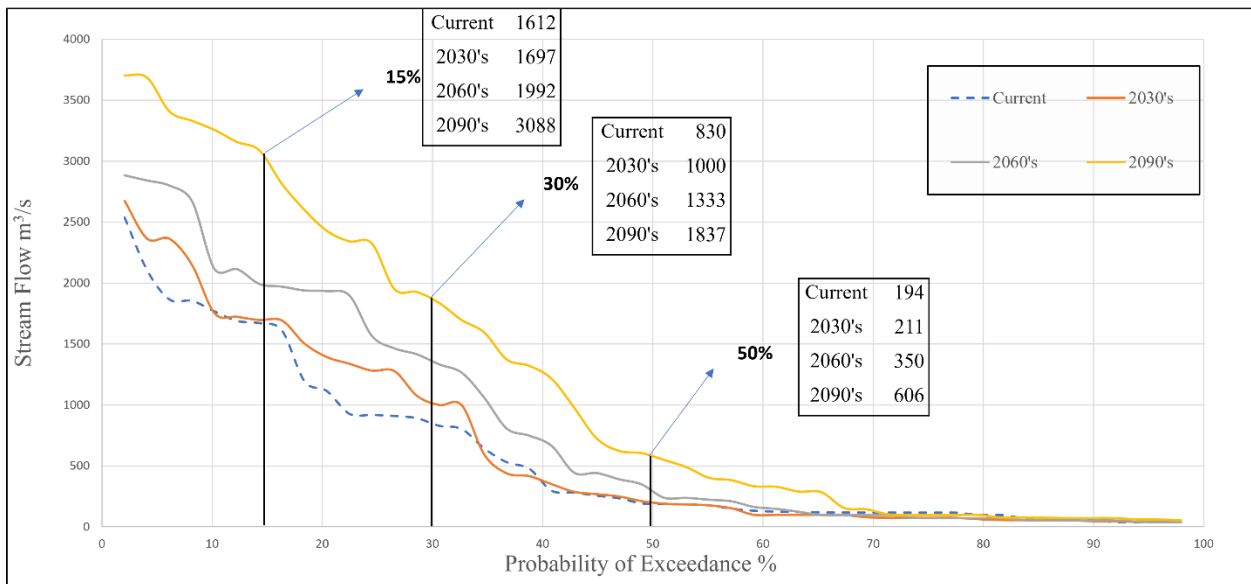


Figure 4.20. Flow duration curve for future stream flows under climate change scenarios SSP5-8.5.

Table 4.5. Expected Hydropower generation under current and future climate change scenario SSP2-4.5.

Scenarios	Q (m ³ /s)	Head (m)	P (kW)	P (MW) at 100% Efficiency	P (MW) at 80% Efficiency	Energy (MWh)	Increase in Power (%)
For 15 % exceedance of the time							
Current	1612	30	473444	473	379	3399331	-
2030's	1700	30	499290	499	399	3584902	5.46
2060's	1701	30	499584	500	400	3587011	5.52
2090's	1841	30	540702	541	433	3882238	14.21
For 30 % exceedance of the time							
Current	830	30	243771	244	195	1750276	-
2030's	1084	30	318371	318	255	2285902	30.60
2060's	1152	30	338342	338	271	2429298	38.80
2090's	1335	30	392090	392	314	2815203	60.84
For 50 % exceedance of the time							
Current	194	30	56978	57	46	409101	-
2030's	213	30	62558	63	50	449167	9.79
2060's	278	30	81649	82	65	586237	43.30
2090's	315	30	92516	93	74	664261	62.37

Table 4.6. Expected Hydropower generation under current and future climate change scenario SSP5-8.5.

Scenarios	Q (m ³ /s)	Head (m)	P (kW)	P (MW) at 100% Efficiency	P (MW) at 80% Efficiency	Energy (MWh)	Increase in Power (%)
For 15 % exceedance of the time							
Current	1612	30	473444	473	379	3399331	-
2030's	1697	30	498437	498	399	3578775	5.28
2060's	1992	30	585161	585	468	4201453	23.60
2090's	3088	30	906986	907	726	6512158	91.57
For 30 % exceedance of the time							
Current	830	30	243709	244	195	1749833	-
2030's	1000	30	293565	294	235	2107800	20.46
2060's	1333	30	391628	392	313	2811890	60.69
2090's	1837	30	539527	540	432	3873802	121.38
For 50 % exceedance of the time							
Current	194	30	56978	57	46	409101	-
2030's	211	30	61972	62	50	444959	8.77
2060's	350	30	102752	103	82	737760	80.34
2090's	606	30	177984	178	142	1277927	212.37

CONCLUSION AND RECOMMENDATIONS

5.1 Conclusion

In the Upper Indus River Basin (UIB) catchments fed by snow and glaciers, the study concludes that the snowmelt runoff model (SRM) founded on a degree day factor is capable of accurately modeling the daily runoff. The SRM is effective in high-altitude catchments because the MOD10A1 satellite-derived cryosphere information has been employed as input to the model for water-equivalent production. This explains the well-known precipitation measurements distortions in rugged watersheds, where snowmelt accounts for a significant portion of river runoff, are not likely to have an impact on the model. Additionally, the Himalayan and Karakoram River basins, where meteorological and hydrological accurate observations are limited or not accessible, can use this product for runoff simulations because this study has used SRM with 0.25x0.25 gridded ECMWF precipitation data (ERA5), which shows the absence of model's sensitive to gridded precipitation dataset. By using the snow cover area whenever it is practical to compute the runoff input, the SRM circumvents the issue of a deficit in precipitation catch (Martinec et al., 2007). During the simulation, SRM has one more distinguishing feature as it takes the precipitation factor two times: firstly, as snow cover input and again as precipitation data input.

The analysis of snow cover area describes that winter months are usually snow covered and have minimal variations in highest elevation zone throughout the year. While other zones have fluctuations in different months of the year. And this variation in snow cover area have highly affected the river runoff.

A quantitative water resources assessment indicates that the months from October to May shows minimal runoff due to very less snow melt in region. As the temperature increases the runoff volume also increases and it shows a maximum discharge of more than $Q = 2300 \text{ m}^3/\text{s}$ in a single day. While average daily run off was found $Q = 571 \text{ m}^3/\text{s}$. The SRM shows exceptionally very good results in both calibration and validation period. The model efficiency results indicated that R^2 was 0.88 for calibration and 0.86 for model validation period. A difference of 2.86% and 1.09% was found in total volume of runoff for model calibration period and for model validation period this difference was 2.91% and 8.97% respectively. The Nash-Sutcliffe efficiency test demonstrated the values of 0.87 and 0.85 for streamflow simulations.

The sensitivity analysis of model shows the DDF and recession coefficients most sensitive for simulations. An increase or decrease of 10% was done to set the parameters to calibrate model. And this manual way of sensitivity analysis was found to be useful for this kind of simulation.

The CMIP6 data for future projections was used under two climate change scenarios SSP2-4.5 and SSP5-8.5. This gave a whole view of future climatic situations up to 2099.

REFERENCES

1. Adnan, M., Nabi, G., Kang, S., Zhang, G., Adnan, R. M., Anjum, M. N., ... & Ali, A. F. (2017). Snowmelt Runoff Modelling under Projected Climate Change Patterns in the Gilgit River Basin of Northern Pakistan. *Polish Journal of Environmental Studies*, 26(2).
2. Adnan, M., Nabi, G., Kang, S., Zhang, G., Adnan, R. M., Anjum, M. N., ... & Ali, A. F. (2017). Snowmelt Runoff Modelling under Projected Climate Change Patterns in the Gilgit River Basin of Northern Pakistan. *Polish Journal of Environmental Studies*, 26(2).
3. Ali, A., Akhtar, R., & Hussain, J. (2023). Unveiling High Mountain Communities' Perception of Climate Change Impact on Lives and Livelihoods in Gilgit-Baltistan: Evidence from People-Centric Approach. *Environmental Communication*, 17(6), 602-617.
4. Ali, S. H., Bano, I., Kayastha, R. B., & Shrestha, A. (2017). Comparative assessment of runoff and its components in two catchments of upper Indus basin by using a semi distributed glacio-hydrological model. *The International Archives of the Photogrammetry, Remote Sensing and Spatial Information Sciences*, 42, 1487-1494.
5. Archer, D. R., Forsythe, N., Fowler, H. J., & Shah, S. M. (2010). Sustainability of water resources management in the Indus Basin under changing climatic and socio economic conditions. *Hydrology and Earth System Sciences*, 14(8), 1669-1680.
6. Azmat, M., Wahab, A., Huggel, C., Qamar, M. U., Hussain, E., Ahmad, S., & Waheed, A. (2020). Climatic and hydrological projections to changing climate under CORDEX-South Asia experiments over the Karakoram-Hindukush-Himalayan water towers. *Science of the Total Environment*, 703, 135010.

7. Buchwitz, M., Reuter, M., Schneising, O., Bovensmann, H., Burrows, J. P., Boesch, H., ... & Schepers, D. (2018). Copernicus Climate Change Service (C3S) global satellite observations of atmospheric carbon dioxide and methane. *Advances in Astronautics Science and Technology*, 1, 57-60.
8. Dyurgerov, M. B., & Meier, M. F. (1997). Mass balance of mountain and subpolar glaciers: a new global assessment for 1961–1990. *Arctic and Alpine Research*, 29(4), 379-391.
9. Haeberli, W., Hoelzle, M., & Suter, S. (1998). Into the second century of worldwide glacier monitoring: prospects and strategies. *Studies and reports in hydrology*, 56.
10. Harrigan, S., Zsoter, E., Alfieri, L., Prudhomme, C., Salamon, P., Wetterhall, F., ... & Pappenberger, F. (2020). GloFAS-ERA5 operational global river discharge reanalysis 1979–present. *Earth System Science Data*, 12(3), 2043-2060.
11. Hayat, H., Akbar, T. A., Tahir, A. A., Hassan, Q. K., Dewan, A., & Irshad, M. (2019). Simulating current and future river-flows in the Karakoram and Himalayan regions of Pakistan using snowmelt-runoff model and RCP scenarios. *Water*, 11(4), 761.
12. Immerzeel, W. W., Droogers, P., De Jong, S. M., & Bierkens, M. F. P. (2009). Large-scale monitoring of snow cover and runoff simulation in Himalayan River basins using remote sensing. *Remote sensing of Environment*, 113(1), 40-49.
13. Krishna, A. P. (2011). Characteristics of snow and glacier fed rivers in mountainous regions with special reference to Himalayan basins. *Encyclopedia of Snow, Ice and Glaciers*, 128-33.
14. Kundzewicz, Z. W., Mata, L. J., Arnell, N. W., Doll, P., Kabat, P., Jimenez, B., ... & Shiklomanov, I. (2007). Freshwater resources and their management.

15. Martinec, J. (1975). Snowmelt-runoff model for stream flow forecasts. *Hydrology Research*, 6(3), 145-154.
16. Martinec, J., & Rango, A. (1986). Parameter values for snowmelt runoff modelling. *Journal of hydrology*, 84(3-4), 197-219.
17. Mukhopadhyay, B., & Khan, A. (2015). A reevaluation of the snowmelt and glacial melt in river flows within Upper Indus Basin and its significance in a changing climate. *Journal of Hydrology*, 527, 119-132.
18. Pokhrel, B. K., Chevallier, P., Andréassian, V., Tahir, A. A., Arnaud, Y., Neppel, L., ... & Budhathoki, K. P. (2014). Comparison of two snowmelt modelling approaches in the Dudh Koshi basin (eastern Himalayas, Nepal). *Hydrological sciences journal*, 59(8), 1507-1518.
19. Rashid, M. U., Ahmed, W., Islam, I., Petrounias, P., Giannakopoulou, P. P., & Koukouzas, N. (2023). Impact of Climate Change on the Stability of the Miacher Slope, Upper Hunza, Gilgit Baltistan, Pakistan. *Climate*, 11(5), 102.
20. Tahir, A. A., Chevallier, P., Arnaud, Y., & Ahmad, B. (2011). Snow cover dynamics and hydrological regime of the Hunza River basin, Karakoram Range, Northern Pakistan. *Hydrology and Earth System Sciences*, 15(7), 2275-2290.
21. Tahir, A. A., Chevallier, P., Arnaud, Y., Neppel, L., & Ahmad, B. (2011). Modeling snowmelt-runoff under climate scenarios in the Hunza River basin, Karakoram Range, Northern Pakistan. *Journal of hydrology*, 409(1-2), 104-117.
22. Tahir, A. A., Chevallier, P., Arnaud, Y., Neppel, L., & Ahmad, B. (2011). Modeling snowmelt-runoff under climate scenarios in the Hunza River basin, Karakoram Range, Northern Pakistan. *Journal of hydrology*, 409(1-2), 104-117.

23. Xie, H., Zhang, G., Yao, T., Li, H., & Duan, S. (2013, December). Quantitative water resources assessment of Qinghai Lake basin using Snowmelt Runoff Model (SRM). In *AGU Fall Meeting Abstracts* (Vol. 2013, pp. GC33B-1122).
24. Xu, C. Y. (1999). Climate change and hydrologic models: A review of existing gaps and recent research developments. *Water Resources Management*, *13*, 369-382.
25. Xu, C. Y. (1999). Climate change and hydrologic models: A review of existing gaps and recent research developments. *Water Resources Management*, *13*, 369-382.
26. Yeleliere, E., Cobbina, S. J., & Duwiejuah, A. B. (2018). Review of Ghana's water resources: the quality and management with particular focus on freshwater resources. *Applied Water Science*, *8*, 1-12.
27. Zhang, G., Xie, H., Yao, T., Li, H., & Duan, S. (2014). Quantitative water resources assessment of Qinghai Lake basin using Snowmelt Runoff Model (SRM). *Journal of Hydrology*, *519*, 976-987.